PETROGRAPHY AND MINERAL COMPOSITIONS OF THE YAMATO-7308 HOWARDITE

Yukio IKEDA

Department of Earth Sciences, Faculty of Science, Ibaraki University, Bunkyo 2-chome, Mito 310

and

Hiroshi TAKEDA

Mineralogical Institute, Faculty of Science, University of Tokyo, 3–1, Hongo 7-chome, Bunkyo-ku, Tokyo 113

Abstract: The constituents of the Y-7308 howardite are classified into four groups: holocrystalline lithic clasts, hypocrystalline to holohyaline materials, mineral fragments and matrix. The holocrystalline lithic clasts include four clans: (1) A diogenitic cumulate type consisting of diogenitic clasts. (2) A eucritic cumulate type consisting of hypersthene-eucritic clasts and coarse-grained inverted pigeonite-eucritic clasts. (3) A Na-rich magma type consisting of fine-grained inverted pigeonite-eucritic clasts. (4) A Na-poor magma type consisting of pigeonite-eucritic clasts and fayalitic olivine-hedenbergitic pyroxene-tridymite-plagiolcase clasts.

Most clasts of hypocrystalline to holohyaline materials were probably formed by shock events from breccias and/or regoliths similar in composition to the whole rock of Y-7308. Most mineral fragments were probably derived by shocks from complete disaggregation of holocrystalline lithic clasts and hypocrystalline to holohyaline materials. Magnesian olivine and orthopyroxene fragments may have been derived from dunitic or orthopyroxenitic rocks whose clasts cannot be observed in Y-7308.

1. Introduction

Howardites are polymict breccias which are similar to lunar breccias and are considered to have been regoliths lithified by intense shocks on the howardite parent body (HPB). They consist of many kinds of clasts derived from the interiors of HPB or formed on the surface by shock events (DUKE and SILVER, 1967; TAKEDA, 1979). The Y-7308 howardite is the most magnesian howardite among all known howardites and seems to include deep components of HPB more abundantly than the others. In addition, Y-7308 comprises unique clasts (Fa-Hd-Trid-Pl clasts) consisting mainly of fayalitic olivine, hedenbergitic pyroxene, tridymite and plagioclase. They are the most ferroan clasts known in howardites, and are considered to be the latest-stage products of fractional crystallization. Therefore, Y-7308 includes lithic clasts ranging from the most magnesian to the most ferroan components known in all howardites.

Detailed studies of Y-7308 may give light on the origin of HPB and the nature of crystallization of howardite-diogenite-eucrite magmas (HED magmas) in addition to the mechanism of regolith formation. In this paper, detailed petrography of Y-7308 and major element compositions of minerals and glasses are presented. A model for the origin of HPB and crystallization of HED magmas will be presented elsewhere.

2. Analytical Methods

Minerals and glasses were analyzed using an electron-probe microanalyzer (EPM-SM type, acceleration voltage was 15 kV, and sample current 5 nA). The correction method for silicates, oxides and glasses is according to BENCE and ALBEE (1968) with revised correction factors of NAKAMURA and KUSHIRO (1970), and that for metals to standard ZAF correction. Bulk compositions of lithic and vitrophyric clasts were obtained using a defocussed beam (about 50 μm in diameter). The correction method for the bulk compositions is according to IKEDA (1980).

3. Constituents

The Y-7308 howardite consists of various kinds of clasts and materials (Figs. 1-1 and 1-2). They are summarized in Table 1.

Table 1. The constituent of the Y-7308 howardite.

Holocrystalline lithic clasts			
	Diogenitic clasts		
	Eucritic clasts		
		Hyp-eucritic clasts	
		IPig-eucritic clasts	Coarse-grained IPig-eucritic clasts
			Fine-grained IPig-eucritic clasts
		Pig-eucritic clasts	
	Fa-Hd-Trid-Pl clasts		
	Magnesian Ol-Px-Pl clasts and magnesian Ol-Px clasts		
Hypocrystalline and holohyaline material			
	Glassy spherules and fragments		
	Vitrophyric clasts		
	Chondrule-like material		
	Shock-darkened or shock-melted material		
Mineral fragments			
	Olivine		
	Pyroxene		
	Plagioclase		
	Chromite		
	Fe-Ni metal		
	Troilite		
Fine-grained matrix			

Holocrystalline lithic clasts are free of any glass except for maskelynites. Diogenitic clasts consist mainly of orthopyroxene aggregates with minor amounts of chromite, troilite, plagioclase (or maskelynite), etc. Eucritic clasts include pyroxene and plagioclase (or maskelynite) as main constituent minerals. They are grouped into three subtypes, hypersthene (Hyp)-eucritic clasts, inverted pigeonite (IPig)-eucritic clasts, and pigeonite (Pig)-eucritic clasts, on the basis that the main low-Ca pyroxenes are primary orthopyroxene, inverted pigeonite or pigeonite, respectively. Magnesian Ol-Px-(Pl) clasts are aggregates of magnesian olivine and orthopyroxene with minor and variable amounts of plagioclase, chromite, etc.

Hypocrystalline to holohyaline materials are glassy spherules, glassy fragments and clasts including glasses or amorphous materials. Glassy spherules are beads of glasses and/or cryptocrystalline materials or their fragments. Glassy fragments are irregular-shaped glassy materials consisting of glasses and/or devitrified glasses, which are probably not fragments of glassy spherules. Vitrophyric clasts consist mainly of laths or quenched crystals of orthopyroxene or olivine and interstitial glasses. They never show spherical outlines and seem to be fragments of larger rocks. Shock-darkened or shock-melted materials are fragments of regoliths, breccias or crystalline rocks which were formed by shock events prior to the formation of Y-7308 breccia. Chondrule-like materials are round objects showing porphyritic textures similar to porphyritic olivine-pyroxene chondrules occurring commonly in unequilibrated chondrites.

Mineral fragments are defined here to be fragments of single crystals with or without exsolution lamellae, larger than about one micron, or fragments of "nearly single crystals" consisting of a main crystal with minor other crystals. Matrix is defined here to be aggregates of fine-grained materials finer than about one micron, and is filling the interstitial spaces among the other components. Matrix is not dealt with in this paper.

4. Holocrystalline Clasts

4.1. Diogenitic clasts

Diogenitic clasts occur commonly as large clasts in Y-7308, and description of typical diogenitic clasts are given as follows. Compositions of silicates and oxides and that of Fe-metals are shown in the Appendix (Tables A-1 and A-12, respectively).

Clast No. 2 (Fig. 1-3) is a largest diogenitic clast, 3.2×1.4 mm in size. It is an aggregate of orthopyroxene grains whose sizes range from a few microns up to 840 μm. The orthopyroxenes are free of any exsolution lamella. They show weak cataclastic texture and heterogeneous extinction, indicating that this clast suffered moderate to intense shock. Accessary minerals are chromite, maskelynite, high-Ca pyroxene, troilite and Fe-metal. Chromite grains, several tens to one hundred microns across, occur commonly. Maskelynite occurs in interstitial spaces between orthopyroxene grains, and rarely small high-Ca pyroxene grains, several tens of microns across, are included in orthopyroxenes. Troilite and Fe-metal are rare.

Clast No. 9 (Fig. 1-4) is 2.8 mm long and 1.2 mm wide. It is an aggregate of equigranular anhedral orthopyroxene grains, about 50 to 350 μm across, with minor amounts of chromite, Fe-metal and troilite. Chromite grains, several to 300 μm in diameter, occur commonly. Round to subangular troilite grains of several to a few ten microns are scattered throughout this clast. Fe-metal is rare.

Clast No. 26, 1.4×0.8 mm in size, is an aggregate of anhedral orthopyroxene grains, several tens of microns across. It includes tiny grains, several to 20 μm across, of troilite, chromite and minor Fe-metal. Diogenitic clast No. 4 (Fig. 1-5) is similar to clast No. 26 in texture.

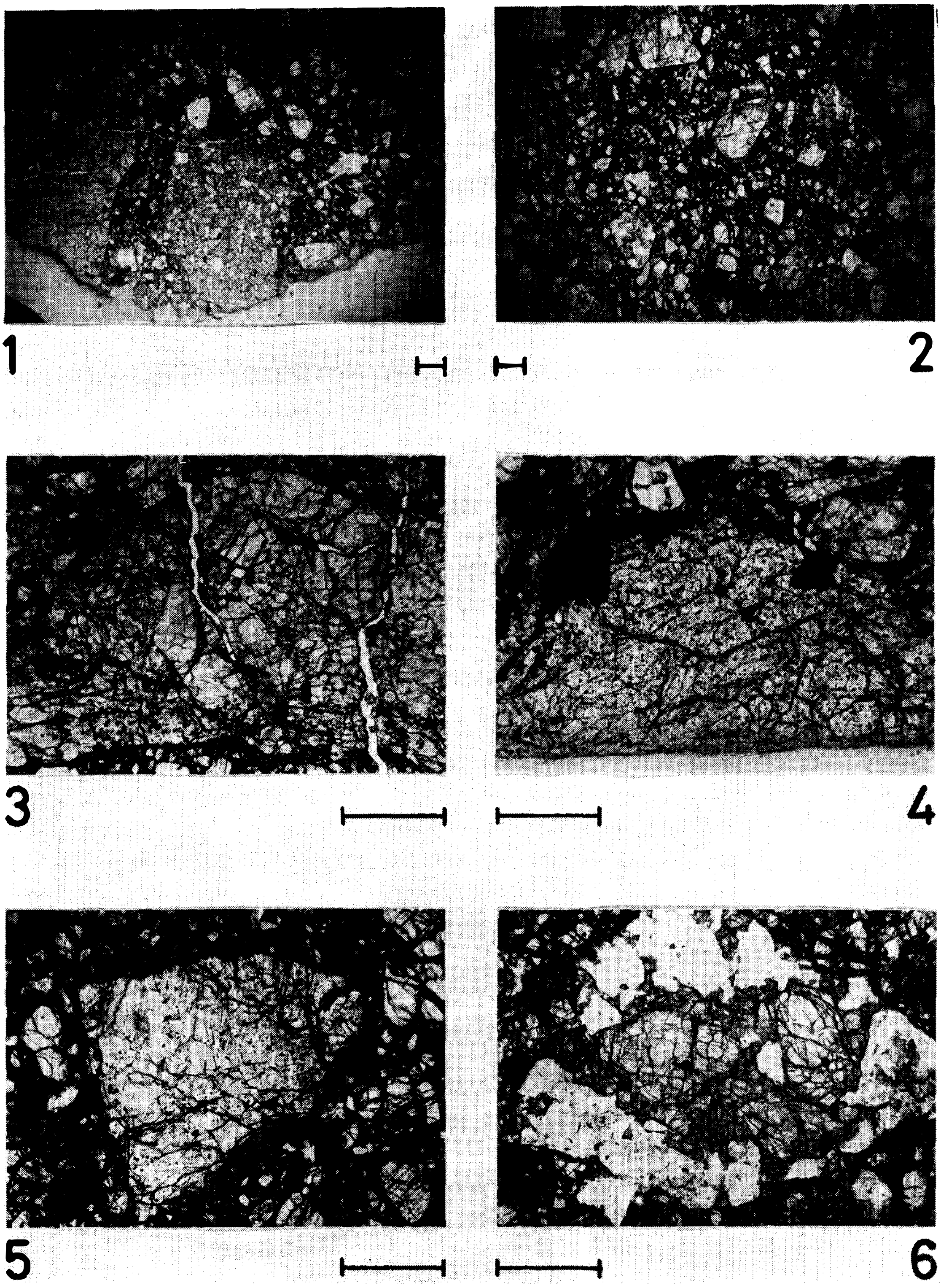

Fig. 1. Photomicrographs of the constituents of Y-7308 (transmitted light). The scale bars are 0.5 mm. Whole views of Y-7308 [1 and 2], diogenitic clasts [3, 4 and 5; clasts Nos. 2, 9 and 4, respectively], Hyp-eucritic clasts [6, 7 and 8 (center); clasts Nos. 6, 31 and 24], coarse-grained IPig-eucritic

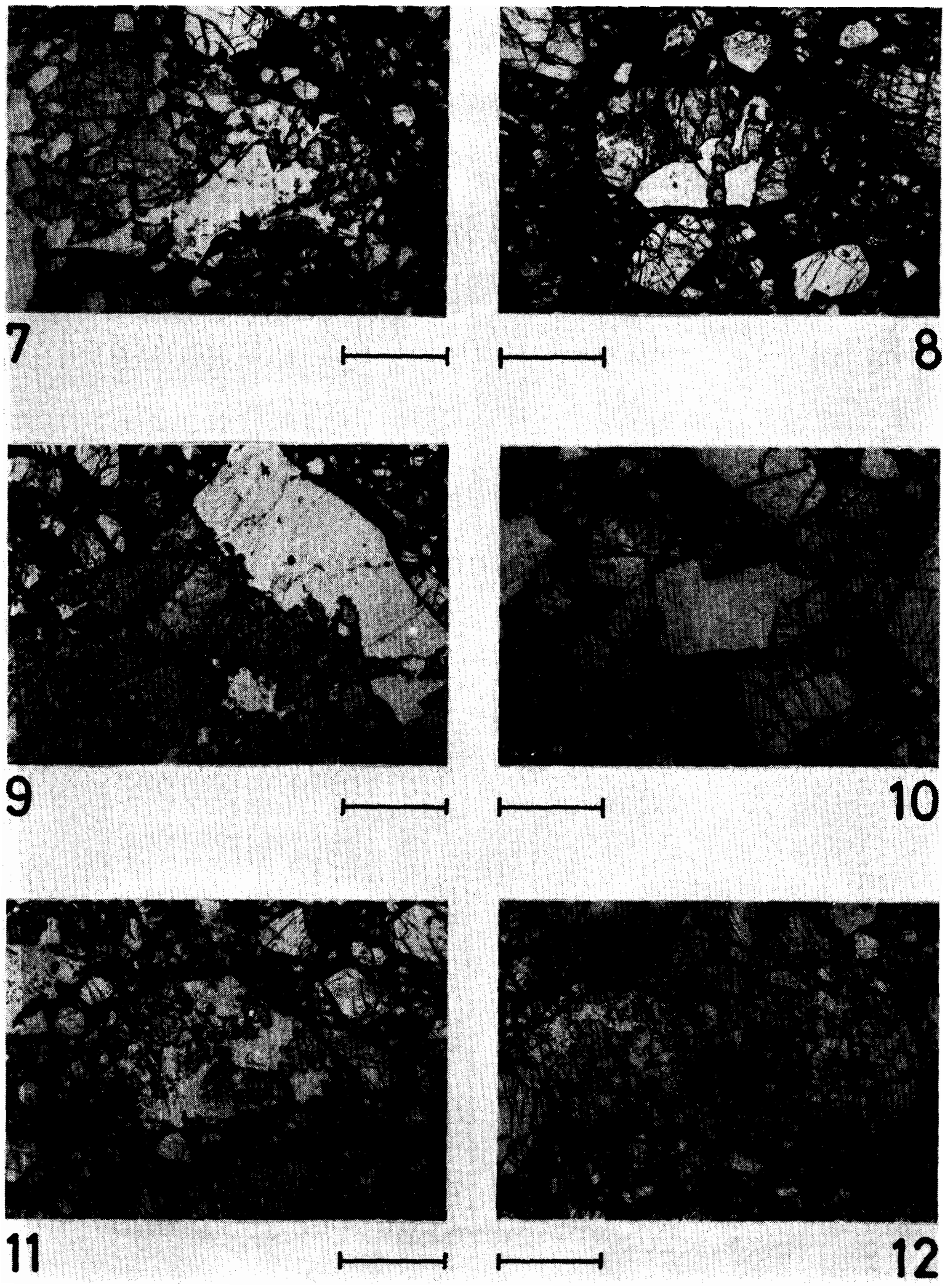

clasts [9 and 10(center); clasts Nos. 3 and 54], fine-grained lPig-eucritic clasts [11(center), 12, 13(center) and 14 (center); clasts Nos. 12, 40, 9′ and 304, a large olivine fragment is in the left side in 14], Pig-eucritic clasts [15, 16 (center), 17 (center) and 18; clasts Nos. 1, 27, 35

13

14

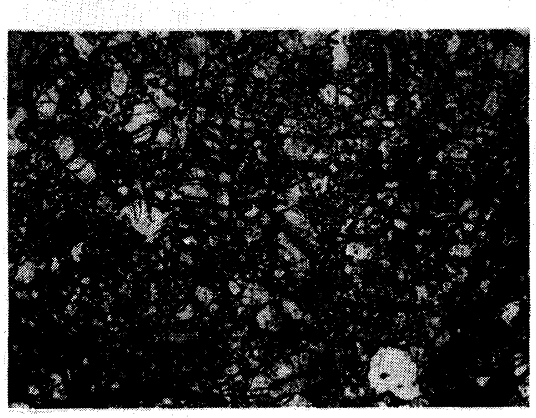

15

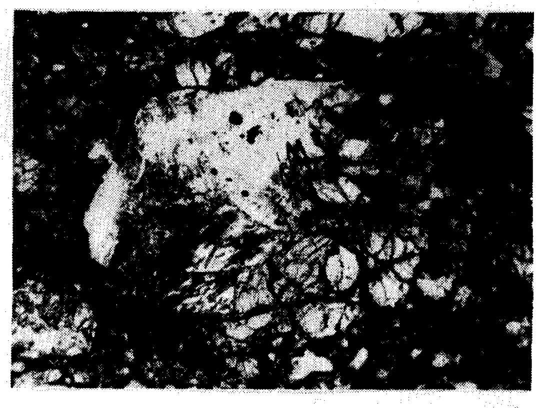

16

17

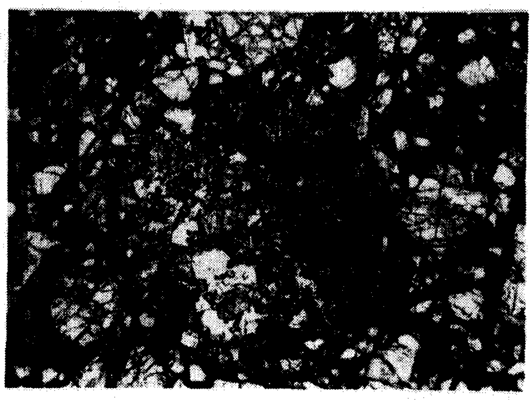

18

and 32], Fa-Hd-Trid-Pl clasts [19 and 20; clasts Nos. 46 and 60], magnesian Ol-Px-Pl clasts [21 (center), 22 (center), 23 (center) and 24 (center); clasts Nos. 87, 91, 526 and 509], glassy spherules and fragments [25, 26, 27 and 28; Nos. 11, 10, 8 and 20 spherules or

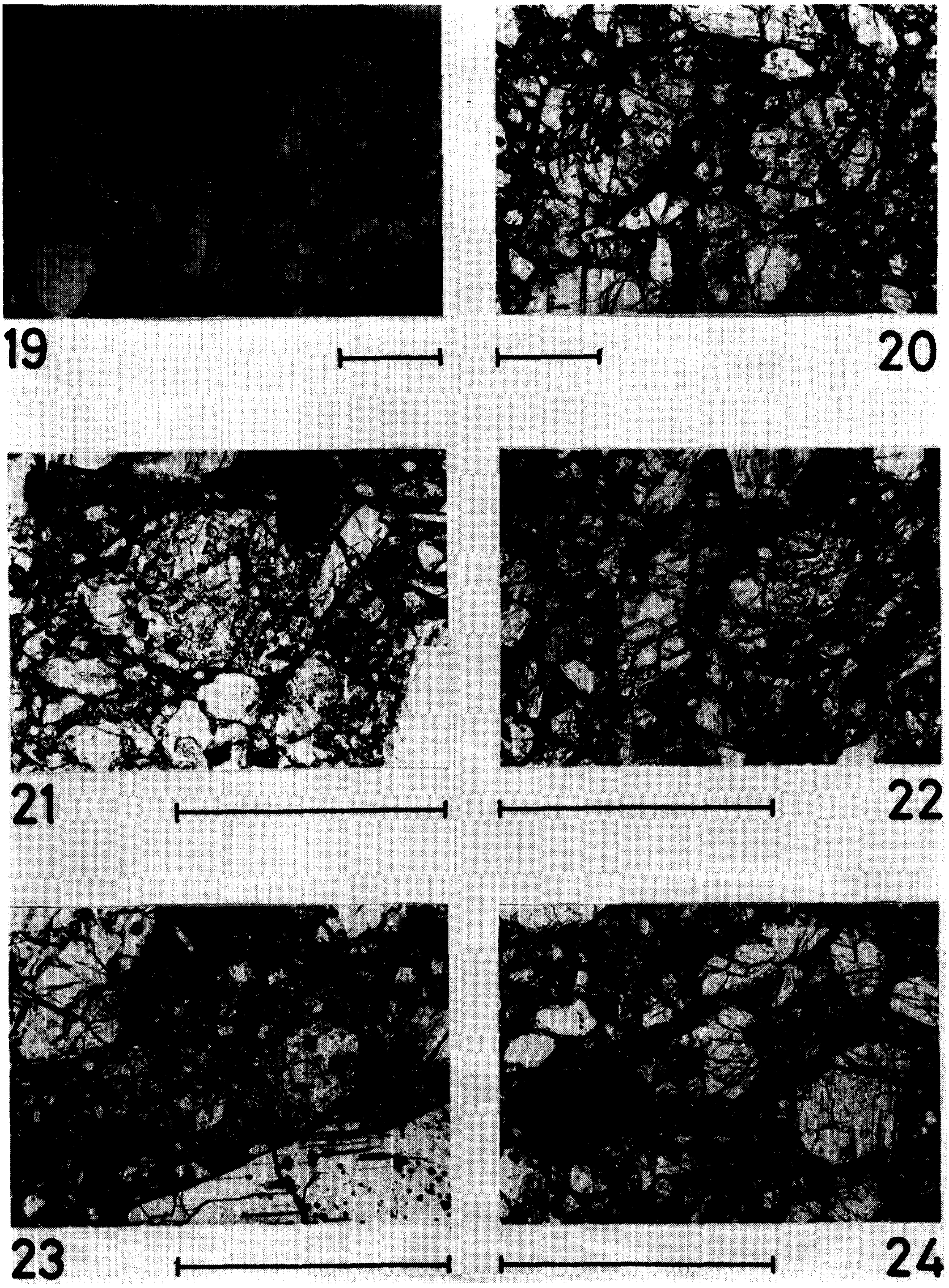

fragments], vitrophyric clasts [29 and 30 (center); clasts Nos. 13 and 28], chondrule-like materials [31 (center) and 32 (center); clasts Nos. 71 and 67], shock-darkened materials [33 (center); clast No. 19], shock-melted materials [34; clast No. 7, central to left side is shock-melt

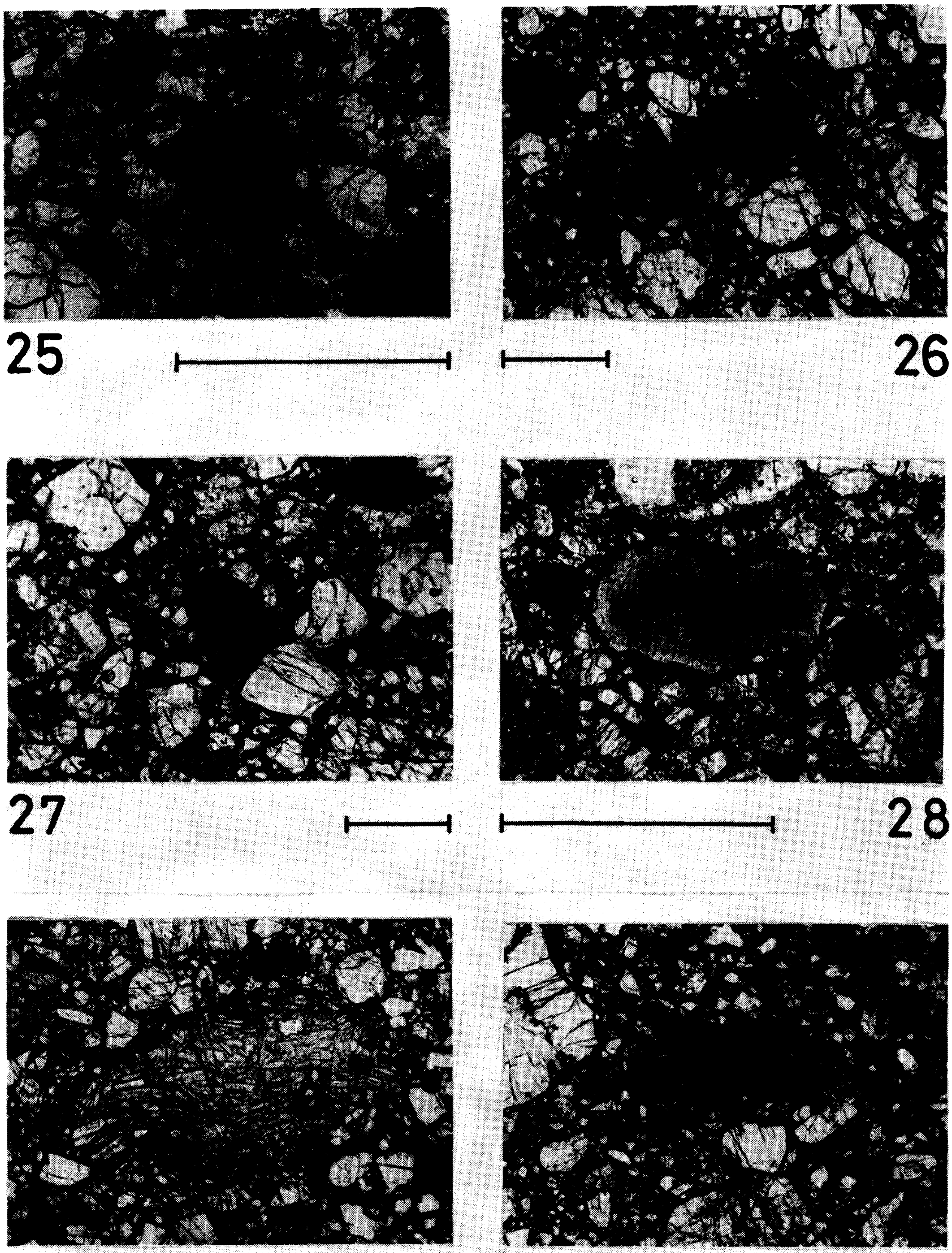

including relic and quenched crystals, and right side is a magnesian Ol-Px clast], olivine fragments [35 (center); No. 47 fragment], orthopyroxene fragments [36 (center), 37 (center) and 38 (center); Nos. 92, 53 and 14 fragments], pigeonite fragments [39; No. 72 fragment],

31

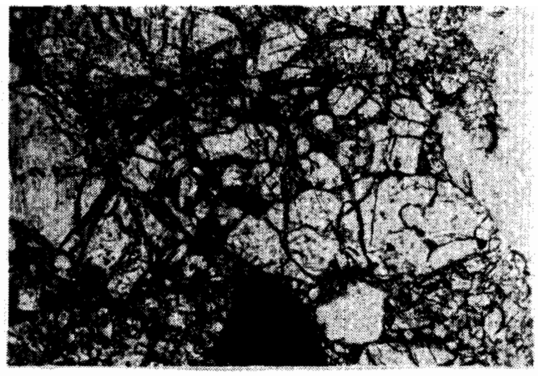

32

33

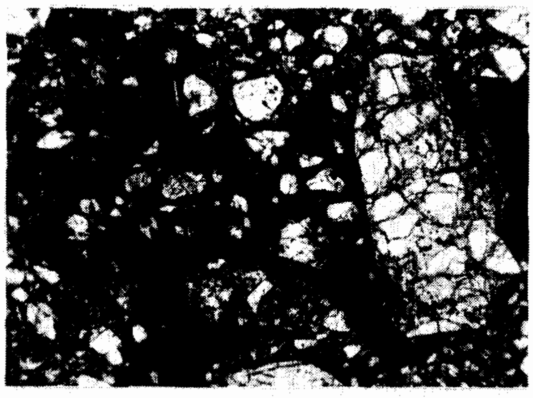

34

35

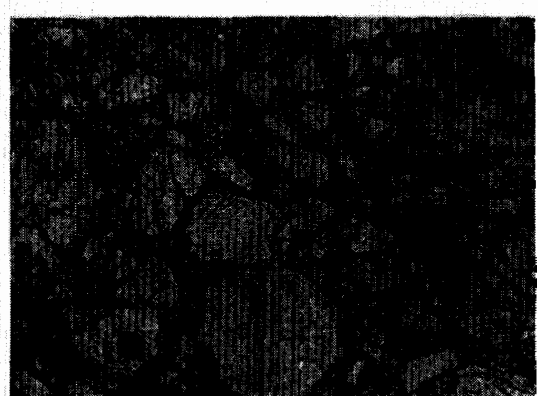

36

Fe-metal fragments [40(center); No. 506 fragment including silicate grains], and plagioclase fragments [41 (center) and 42 (center), No. 70 including blebs of SiO_2 mineral and No. 16 fragments].

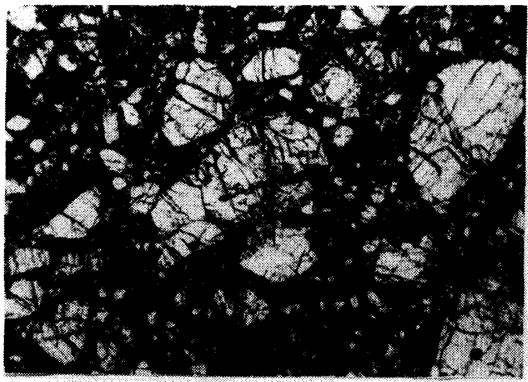

37

38

39

40

41

42

4.2. *Hyp-eucritic clasts*

These clasts are of a unique type which has not been reported in other howardites. Compositions of the constituent minerals are shown in the Appendix (Table A-2).

Clast No. 6 (Fig. 1-6), 2.4×1.4 mm, is a coarse-grained clast consisting of plagioclase and pyroxene with minor amounts of chromite, troilite and Fe-metal. Plagioclases are several hundred microns in size and show heterogeneous to wavy extinction, indicating that this clast suffered weak to moderate shock. Pyroxenes are orthopyroxene whose grain sizes range up to 800 μm across. Large orthopyroxene grains include worm-like small high-Ca pyroxene inclusions. Chromites smaller than 40 μm occur in pyroxene grains or between pyroxene and plagioclase grains. Troilites up to several tens of microns occur with rare Fe-metal grains.

Clast No. 31 (Fig. 1-7) consists of pyroxene and maskelynite with minor chromite. Low-Ca pyroxenes seem to be originally orthopyroxene but show heterogeneous extinction, indicating that this clast suffered moderate to intense shock. Minor small granular high-Ca pyroxenes are included in low-Ca pyroxenes. Clast No. 24 (Fig. 1-8) is similar to clast No. 31 in texture.

4.3. *IPig-eucritic clasts*

IPig-eucritic clasts are subdivided into two subtypes, coarse-grained and fine-grained, depending on whether they contain plagioclase (or maskelynite) grains whose width is larger than several hundred microns. The former shows coarse-grained gabbroic textures and the latter often ophitic to subophitic textures. Compositions of the constituent minerals in IPig-eucritic clasts are tabulated in the Appendix (Tables A-3 and A-12).

Clast No. 3 (Fig. 1-9) is a coarse-grained IPig-eucritic clast consisting of pyroxene and maskelynite with minor chromite. Low-Ca pyroxenes show heterogeneous extinction, indicating moderate to intense shock. Low-Ca pyroxenes sometime include (001) lamellae of high-Ca pyroxenes. A large maskelynite, 1.4×0.6 mm, occurs at the edge of the clast, but small maskelynite grains are included in pyroxenes. Chromite grains, several to 80 μm across, occur mainly as inclusions in pyroxenes.

Clast No. 54 (Fig. 1-10) is a coarse-grained IPig-eucritic clast, 0.85×0.57 mm, consisting of plagioclase, pyroxene, chromite and minor Fe-metal. A large plagioclase grain occupies about 60–70% in area. Pyroxenes are orthopyroxene including (001) lamellae or rods of high-Ca pyroxene. A large chromite grain, 400×150 μm, occurs at the edge of this clast.

Clast No. 12 (Fig. 1-11) is a fine-grained IPig-eucritic clast, showing subophitic texture. It consists of pyroxene, plagioclase, and crystobalite with minor amounts of chromite, Fe-metal and troilite. Pyroxene grains are orthopyroxene with (001) lamellae and discrete high-Ca pyroxene. Plagioclases show euhedral lath-shapes and are narrower than about 200 μm in width. Crystobalite occurs in interstitial spaces surrounded by plagioclase and pyroxene grains. Chromite, Fe-metal and troilite occur mainly as inclusions in pyroxenes. Remarkable shock effects are not observed in this clast.

Clast No. 40 (Fig. 1-12) is a fine-grained IPig-eucritic clast showing ophitic to subophitic texture. It consists of plagioclase and pyroxene with chromite, ilmenite, Fe-metal and minor troilite. Plagioclases often show lath-shapes and locally include many small blebs of pyroxenes, several microns across. Pyroxene grains are orthopyroxenes with (001) lamellae and discrete high-Ca pyroxenes. Fe-metal grains, less than 50 μm across, occur commonly. Chromites occur together with ilmenites.

Clasts Nos. 9′ (Fig. 1-13) and 304 (Fig. 1-14) and other clasts (Nos. 65, 68, 301 and 304) belong to fine-grained type of IPig-eucritic clasts.

4.4. *Pig-eucritic clasts*

These clasts occur commonly as small clasts except one (clast No. 1). Compositions of the constituent minerals are shown in the Appendix (Tables A-4 and A-12).

Clast No. 1 (Fig. 1-15) consists of pyroxene and plagioclase with chromite, troilite and Fe-metal. The texture of this clast resembles that of the Ibitira meteorite (STEELE and SMITH, 1976). Plagioclases show two modes of occurrence. Some occur as interstitial minerals or small euhedral crystals between pyroxene grains. Others occur as large single crystals of subround shapes, 200 to 600 μm across. Pyroxenes are mainly pigeonites with (001) lamellae, and minor granular high-Ca pyroxenes occur between pigeonite and plagioclase. Chromite and ilmenite, smaller than 80 μm across, occur in intimate association. The bulk compositions of the whole clast and a pigeonite grain with lamellae are also shown in the Appendix (Table A-4).

Clast No. 27 (Fig. 1-16) consists of plagioclase and pyroxene with chromite, troilite and Fe-metal. Plagioclases include locally many tiny rods of high-Ca pyroxenes, up to 150×15 μm. Pyroxenes are high-Ca pyroxenes and pigeonites with (001) lamellae.

Clast No. 35 (Fig. 1-17) consists of plagioclase and pyroxene with ilmenite and chromite. One plagioclase grain includes small blebs of an SiO_2-mineral and pyroxene. Pyroxenes are high-Ca pyroxene and pigeonite. Ilmenite, up to 80 μm across, occurs in contact with chromite grains.

Clast No. 32 (Fig. 1-18) consists of plagioclase and pyroxene with ilmenite and chromite. One half of the clast shows a granular texture consisting of subround grains of pyroxene and plagioclase, but the other half shows ophitic to quenched texture consisting of needles or long laths of plagiolcase and larger laths of pyroxene.

4.4. *Fa-Hd-Trid-Pl clasts*

These are of a unique type which has not been repoted in other howardites, but NEHRU *et al.* (1983) reported a clast of this type in Y-7308. Only two clasts of this type were observed in our thin sections. Compositions of the constituent minerals are shown in the Appendix (Table A-5).

Clast No. 46 (Fig. 1-19) consists of fayalitic olivine, hedenbergitic pyroxene, tridymite and plagioclase with minor amounts of ilmenite, chromite, troilite, Fe-metal and whitlockite. Fayalitic olivines are euhedral to subhedral grains, several tens of microns across, and sometimes included in hedenbergitic pyroxenes. Hedenbergitic pyroxenes are coarser than olivine grains and are free of any exsolution lamella or bleb. Plagioclases and tridymites are coarse-grained, about several hundred microns across. A large ilmenite grain of about 200 μm including a thin film of chromite occurs in plagioclase. Clast No. 60 (Fig. 1-20) consists of hedenbergitic pyroxene, fayalitic olivine, tridymite, plagioclase and ilmenite. Fayalitic olivines, several tens of microns across, are corroded forms and included in hedenbergitic pyroxenes.

4.5. Magnesian Ol-Px-Pl clasts and magnesian Ol-Px clasts

The clasts are rare and occur as small clasts except one (clast No. 7). Compositions of the constituent minerals are shown in the Appendix (Table A-6).

Clast No. 87 (Fig. 1-21) is a magnesian Ol-Px-Pl clast consisting of olivine, orthopyroxene, plagioclase and chromite. Olivine is the largest crystal, 250×70 μm, occurring at the edge of the clast. The main part of the clast is occupied by an aggregate of orthopyroxene. Many irregular blebs of plagioclase, less than 25 μm across, are included in pyroxenes. The bulk composition of the whole clast is also shown in the Appendix (Table A-6).

Clast No. 91 (Fig. 1-22) is a magnesian Ol-Px-Pl clast consisting of olivine and orthopyroxene with minor amounts of high-Ca pyroxene and plagioclase. Clasts Nos. 526 (Fig. 1-23) and 509 (Fig. 1-24) show textures similar to that of clast No. 87 and belong to magnesian Ol-Px-Pl clasts.

Clast No. 7 consists of two lithologies, shockmelt part and unmelted part, as shown in Fig. 1-34. The unmelted part of the clast is a magnesian Ol-Px clast consisting of olivine and orthopyroxene with minor chromite.

5. Hypocrystalline to Holohyalline Materials

5.1. Glassy spherules and fragments

Y-7308 includes glassy spherules (Fig. 1-25) and their fragments (Figs. 1-26 and 1-27), a few hundred microns in radius. In addition, irregular-shaped glassy fragments (Fig. 1-28) sometimes occur. Glassy spherules and their fragments are often cryptocrystalline showing excentro-radial textures, although irregular-shaped glassy fragments do not show those textures. Compositions of glassy spherules and irregular-shaped glassy fragments are shown in the Appendix (Table A-7).

5.2. Vitrophyric clasts

These clasts show always irregular outlines and are fragments of larger glassy materials including microphenocrysts or quenched crystals. Compositions of minerals and glasses are shown in the Appendix (Table A-8).

Clast No. 13 (Fig. 1-29) is a vitrophyric clast consisting of pyroxene laths and interstitial green glass. The length and width of laths range up to 280 and 60 μm, respectively. They are orthopyroxenes, and are rarely rimed with thin pigeonite veneers. An irregular small inclusion, 150×200 μm in size, occurs in this clast. The inclusion comprises olivine, a SiO_2-mineral and fine-grained materials. The compositions of the olivine and the SiO_2-mineral in the irregular inclusion are shown in the Appendix (Table A-8), where the bulk composition of the whole clast is also given.

Clast No. 28 (Fig. 1-30) is another vitrophyric clast including quenched orthopyroxene crystals and black groundmass glass. Small needle crystals of olivine occur in the the groundmass. Clast No. 58 is a small glass clast, 160×270 μm, including euhedral olivine crystal of 80×140 μm.

5.3. Chondrule-like materials

Clast No. 71 (Fig. 1-31) shows a circular shape of about 550 μm in diameter, one fifth of which is broken off. This clast shows a microporphyritic texture, consisting of pyroxene, olivine and devitrified groundmass glass. Pyroxenes are euhedral to subhedral crystals, several tens of microns in width. Most pyroxenes are orthopyroxene with pigeonite rims, but others show polysynthetic twinning and, oblique extinction, indicating that they are low-Ca clinopyroxene. Compositions of olivine and pyroxene are shown in the Appendix (Table A-9) together with the bulk composition of the whole clast. Clast No. 67 (Fig. 1-32) is similar to clast No. 71 in texture, except that the crystallinity of the groundmass is higher. Compositions of olivine and orthopyroxene are shown in the Appendix (Table A-9).

5.4. *Shock-darkened or shock-melted materials*

Clast No. 19 (Fig. 1-33) is a shock-darkened clast consisting of fine-grained darkened materials and irregular relic minerals. Clast No. 7 (Fig. 1-34) includes a shock-melted part and an unmelted part. The shock-melted part consists of irregular-shaped relic minerals, quenched crystals and black glass. Compositions of relic minerals are nearly the same as those of minerals in the unmelted part, whereas those of quenched minerals are magnesian. Their compositions are shown in the Appendix (Table A-10).

6. Mineral Fragments

6.1. *Olivine fragments*

Olivine fragments (Figs. 1-35 and 1-14) occur commonly in Y-7308. Their sizes range up to 0.5 mm. Their compositions are shown in the Appendix (Table A-11). Large olivines, 300–500 μm across, range from Fo_{88} to Fo_{71} in composition, although olivine fragments smaller than about 200 μm are Fo_{77} to Fo_{70}. A large olivine fragment (No. 63) includes Fe-metal, the composition of which is shown in the Appendix (Table A-12).

6.2. *Pyroxene fragments*

Pyroxene fragments occur abundantly, and their sizes are up to about 1.2 mm. They are orthopyroxene, inverted pigeonite, pigeonite with or without lamellae and high-Ca pyroxene. Their compositions are shown in the Appendix (Table A-11) together with those of included minor minerals.

Pyroxene fragment No. 90 is an orthopyroxene lath, 120×70 μm, including a small corroded olivine grain, and resembles orthopyroxene laths in chondrule-like materials. Pyroxene fragment No. 92 (Fig. 1-36) is orthopyroxene, and a small olivine grain is attached at one corner of the pyroxene fragment. Pyroxene fragment No. 53 (Fig. 1-37) is a large orthopyroxene including small blebs (about 20–30 μm across) of plagioclase, high-Ca pyroxene and troilite. Fragment No. 14 (Fig. 1-38) is a large orthopyroxene with many inclusions of troilite smaller than 40 μm. Fragment No. 72 (Fig. 1-39) is a pigeonite grain with (001) lamellae. The compositions of the bulk grain and the host pigeonite are shown in the Appendix (Table A-11).

6.3. *Plagioclase fragments*

Plagioclase fragments (Figs. 1-41 and 1-42) also occur commonly in Y-7308. Their sizes range up to about 1 mm. They sometimes show heterogeneous extinction, indicating moderate to intense shock, although some plagioclase fragments are free of any detectable shock. Compositions of the plagioclase fragments are shown in the Appendix (Table A-11). They rarely include small blebs of SiO_2-minerals (Fig. 1-41) or high-Ca pyroxenes, the compositions of which are also shown in the Appendix (Table A-11).

6.4. Chromite, Fe-metal and troilite fragments

Chromite fragments occur commonly. Their compositions are shown in the Appendix (Table A-11).

Fe-metals and troilites occur in lithic clasts and also as mineral fragments. Compositions of Fe-metal fragments are shown in the Appendix (Table A-13). Fragment No. 506 (Fig. 1-40) is Fe-metal including pyroxene and SiO_2-mineral grains. Fragment No. 69 (Fig. 1-33, upper central) is a troilite grain including orthopyroxene and high-Ca pyroxene. The high-Ca pyroxene is the most magnesian high-Ca pyroxene in Y-7308.

7. Discussion

7.1. Holocrystalline lithic clasts

Some diogenitic clasts such as clast No. 2 show cataclastic textures, indicating that they were originally coarse-grained rocks. The other diogenitic clasts such as Nos. 9, 26 and 4 have finer grain sizes than clast No. 2 and show mosaic textures of intimately interlocking aggregates of anhedral pyroxene grains. These textures might be formed from coarse-grained diogenitic rocks by shocks and subsequent recrystallization. Compositions of orthopyroxenes in diogenitic clasts are plotted in Fig. 2a, ranging from $En_{75}Fs_{23.5}Wo_{1.5}$ to $En_{66}Fs_{31.5}Wo_{2.5}$, and show nearly the same range as orthopyroxenes in all known diogenities (TAKEDA, 1979). The Al_2O_3 and Cr_2O_3 contents of orthopyroxenes in diogenitic clasts are high in comparison with those in eucritic clasts although the TiO_2 contents are low in diogenitic clasts (Fig. 3). Chromites in diogenitic clasts are low in TiO_2 and range from $Chr_{67}Sp_{30}Us_3$ to $Chr_{80}Sp_{19}Us_1$ (Fig. 4). Composition of maskelynite in the most ferroan diogenitic clast is $An_{95.5}Ab_{4.5}$. Fe-metals in diogenitic clasts have the Co contents ranging from 0.68 to 2.4 wt% (Fig. 5a).

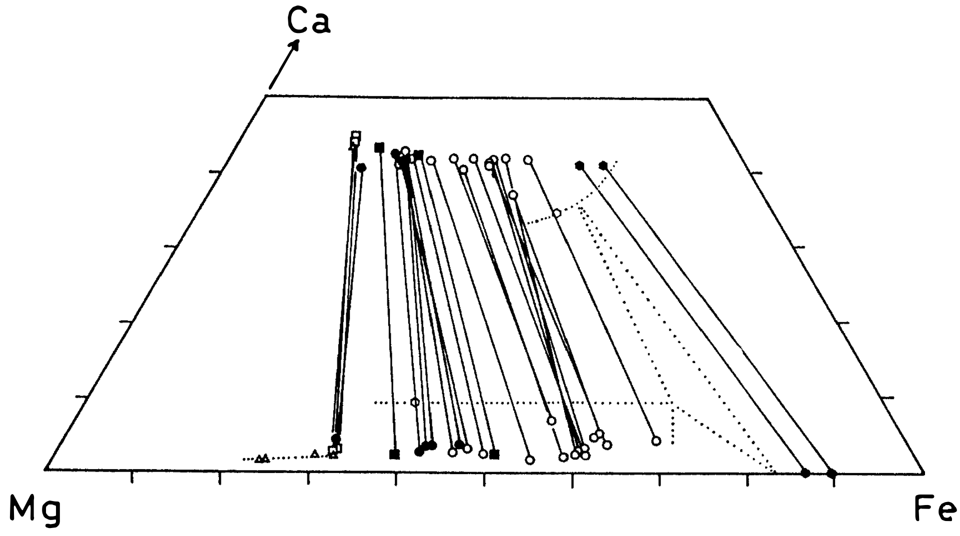

Fig. 2a.

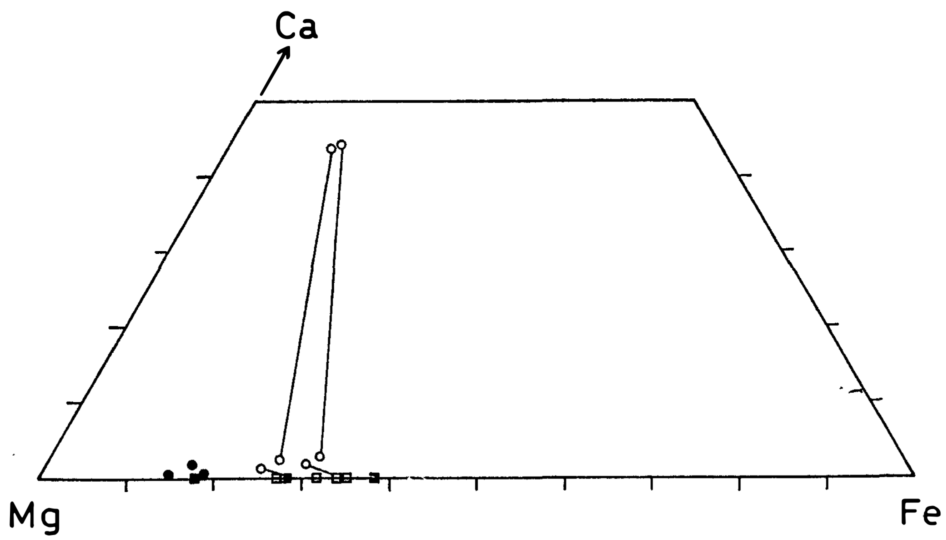

Fig. 2b.

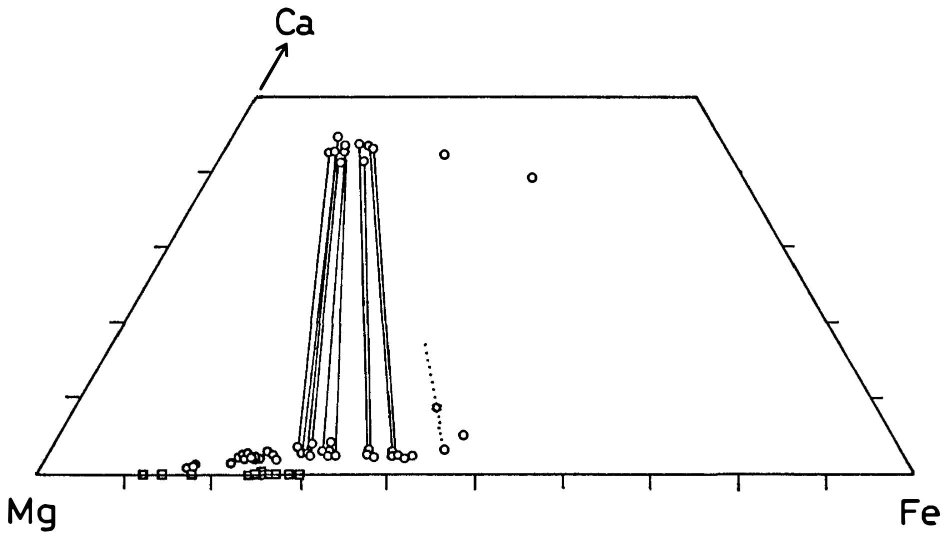

Fig. 2c.

Fig. 2. Compositions (in atomic ratio) of pyroxenes and olivines.

a. Low-Ca pyroxenes and coexisting high-Ca pyroxenes connected by tie lines, in diogenitic clasts (△), Hyp-eucritic clasts (□), coarse-grained IPig-eucritic clasts (■) fine-grained IPig-eucritic clasts (●), Pig-eucritic clasts (○), and Fa-Hd-Trid-Pl clasts (●, high-Ca pyroxenes and fayalitic olivines). Two open hexagons are bulk-grain compositions of an inverted pigeonite in an IPig-eucritic clast and a high-Ca pyroxene in a Pig-eucritic clast. Dotted lines show compositional trends of orthopyroxenes, primary pigeonites and primary high-Ca pyroxenes together with a three-phase triangle.

b. Pyroxenes (circles) and olivines (squares) in magnesian Ol-Px-(Pl) clasts (open marks) and chondrule-like material (solid marks).

c. Pyroxene fragments (○), olivine fragments (□), and bulk grain of a pigeonite fragment with lamellae (⬡).

Hyp-eucritic clasts also suffered shock effects and were probably derived from coarse-grained plagioclase-orthopyroxene eucritic rocks. The compositions of orthopyroxenes are $En_{65-66}Fs_{31-32}Wo_{2-3}$ (Fig. 2a), and nearly coincide with those of orthopyroxenes in the most ferroan diogenitic clasts. High-Ca pyroxenes are En_{42-43}

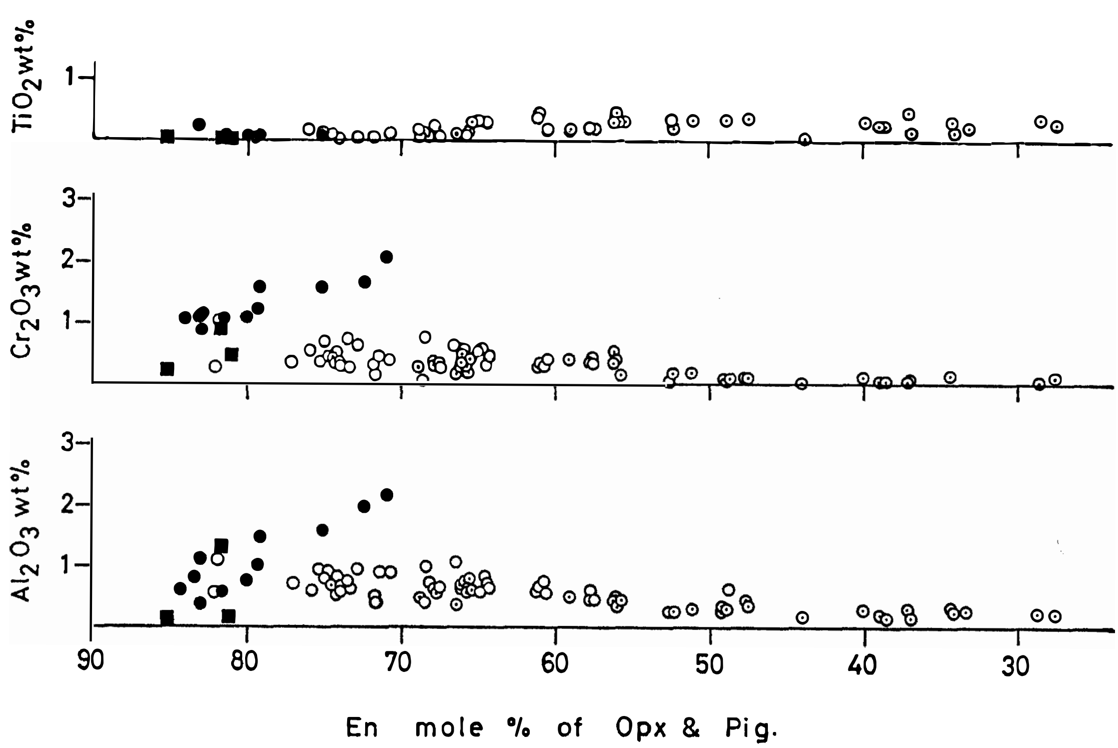

Fig. 3. Al_2O_3, Cr_2O_3 and TiO_2 contents of low-Ca pyroxenes in holocrystalline lithic clasts (⊙), vitrophyric clasts (●), chondrule-like material (■), and occurring as mineral fragments (○).

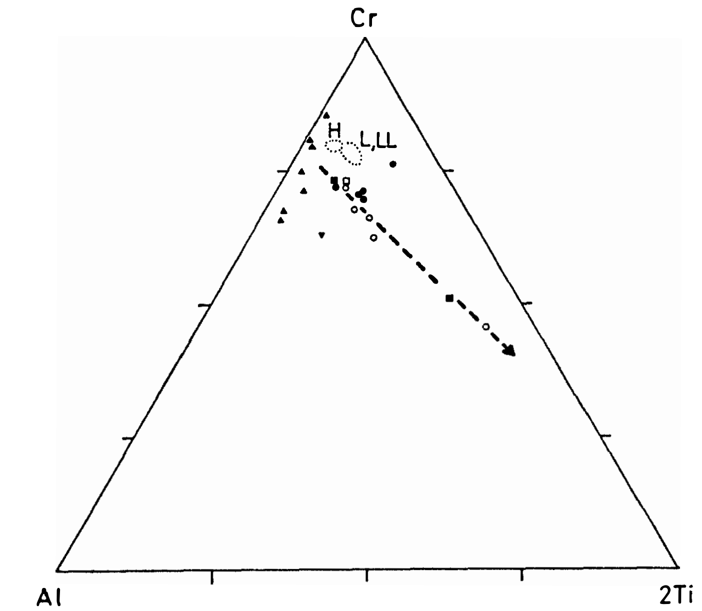

Fig. 4. Compositions (in atomic ratio) of chromites in holocrystalline lithic clasts and occurring as fragments. Symbols are the same as in Fig. 2a. Solid triangles and reverse open triangles are fragments and magnesian Ol-Px-Pl clasts, respectively. Two fields denoted by H and L,LL are compositional ranges of chromites in equilibrated H and L(LL) chondrites (IKEDA, unpublished data).

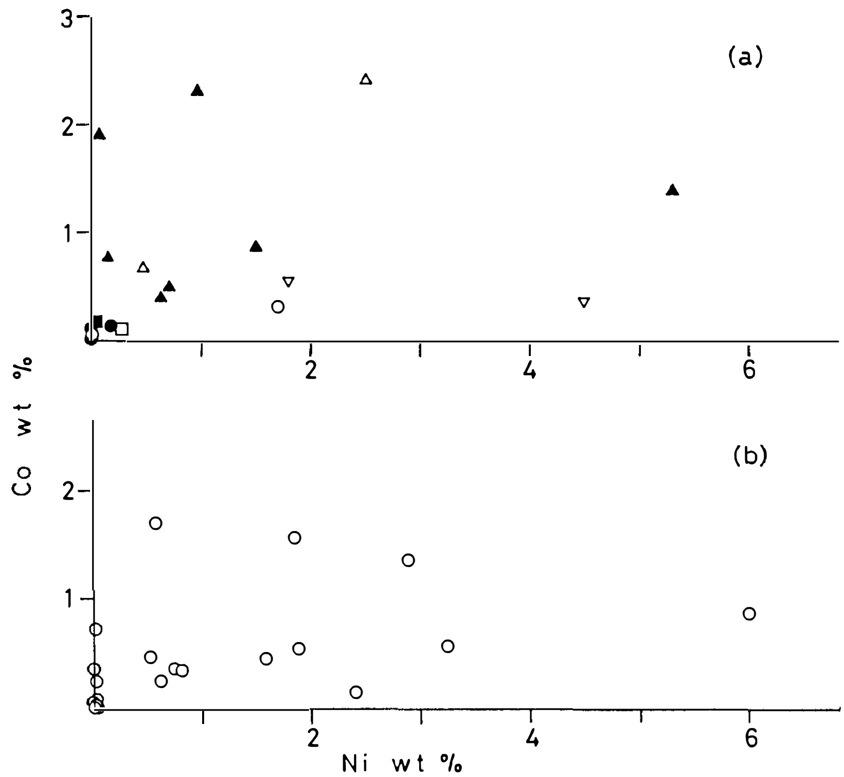

Fig. 5. Co and Ni contents of Fe-metals. a. Fe-metals in holocrystalline lithic clasts and in pyroxene fragments. Symbols are the same as in Fig. 2a, and solid triangles and reverse open triangles are Fe-metals in pyroxene fragments and magnesian Ol-Px-Pl clasts, respectively. b. Fe-metals occurring as mineral fragments.

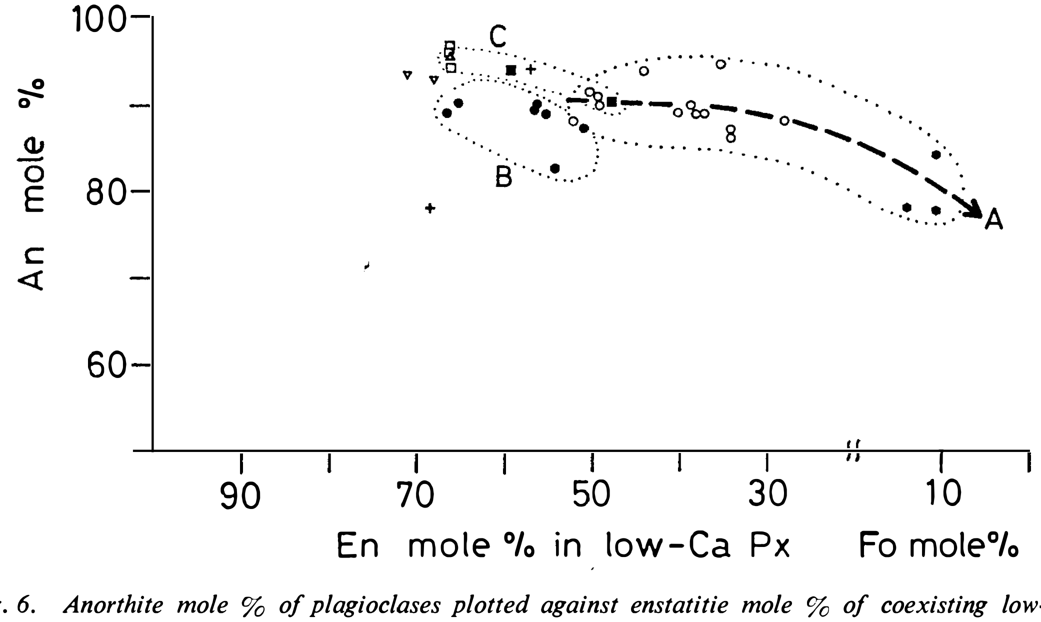

Fig. 6. Anorthite mole % of plagioclases plotted against enstatitie mole % of coexisting low-Ca pyroxenes or forsterite mole % of coexisting fayalitic olivines. Symbols are the same as in Fig. 2a, and reverse open triangles and crosses are magnesian Ol-Px-Pl clasts and orthopyroxene fragments including small blebs of plagioclase, respectively.

$Fs_{12-13}Wo_{44-45}$ and slightly more calcic than those ($En_{43.5}Fs_{13}Wo_{43.5}$) in the most ferroan diogenitic clast (Fig. 2a). Compositions of plagioclases or maskelynites in Hyp-eucritic clasts are $An_{94-96}Ab_{4-6}$. In Fig. 6, anorthite mole % of plagioclases or maskelynites is plotted against enstatitie mole % of coexisting low-Ca pyroxenes. Plagioclases and maskelynites in Hyp-eucritic clasts are plotted in the same area as those in diogenitic clasts. Chromite in a Hyp-eucritic clast is $Chr_{73}Sp_{17}Us_{10}$, richer in TiO_2 than those in diogenitic clasts (Fig. 4).

The coarse-grained IPig-eucritic clasts show gabbroic textures and consist of inverted pigeonite, plagioclase or maskelynite, and chromite with minor Fe-metal. On the other hand, the fine-grained IPig-eucritic clasts sometimes show ophitic to subophitic textures and consist of inverted pigeonite, high-Ca pyroxene, plagioclase, chromite, ilmenite, crystobalite, Fe-metal and/or troilite. The inverted pigeonites of the coarse-grained type include wide (001) lamellae of high-Ca pyroxenes, and those of the fine-grained type include narrow (001) lamellae or blebs of high-Ca pyroxenes. Compositions of pyroxenes are homogeneous in the coarse-grained type whereas those in the fine-grained type sometimes show slight zoning from magnesian core to ferroan rim. Compositions of orthopyroxenes in the coarse-grained type are $En_{47.5-59}Fs_{38.5-50}Wo_{2.5}$, and those in the fine-grained type range from $En_{65}Fs_{31}Wo_4$ to $En_{51}Fs_{45.5}Wo_{3.5}$ (Fig. 2a). The Wo contents of orthopyroxenes in the coarse-grained type are lower than those in the fine-grained type, whereas the Wo contents of coexisting high-Ca pyroxenes (Wo_{42-43}) are higher in the former than in the latter ($Wo_{40.5-42.5}$). The Wo contents of primary pigeonites in the fine-grained type are about 9. Plagioclases or maskelynites in the coarse-grained type are $An_{90-94}Ab_{6-10}$, and those in the fine-grained type are slightly more sodic than those in the coarse-grained type, and seem to form a cluster denoted by B in Fig. 6. On the other hand, plagioclases and maskelynites in the coarse-grained type seem to form a calcic trend denoted by C in Fig. 6 together with those in the Hyp-eucritic clasts. Chromites in the coarse-grained type range from $Chr_{73}Sp_{18.5}Us_{8.5}$ to $Chr_{51}Sp_{11}Us_{38}$ (Fig. 4). Those in the fine-grained type are $Chr_{70-72.5}Sp_{15-18.5}Us_{9-15}$, nearly the same as those in magnesian clasts of the coarse-grained type. Fe-metals in IPig-eucritic clasts are poorer in Ni and Co than those in diogenitic clasts (Fig. 5a), although Fe-metals in the coarse-grained type are slightly richer in Co than those in the fine-grained type.

These differences in textures and mineral compositions between the coarse-grained and fine-grained types of IPig-eucritic clasts suggest that the former type was formed in slow-cooling conditions as coarse-grained gabbroic rocks such as cumulates in magma reservoirs or oceans, whereas the latter type represents magmas solidified in rapid-cooling conditions.

Pig-eucritic clasts have fine grain sizes and sometimes show ophitic to subophitic textures similar to the fine-grained IPig-eucritic clasts. They are free of detectable shock effect, and may have been originally fine-grained. Primary pyroxenes in magnesian Pig-eucritic clasts are pigeonite and subordinate high-Ca pyroxene, although ferroan Pig-eucritic clasts include primary high-Ca pyroxenes more abundantly. Most pigeonites include exsolution lamellae of high-Ca pyroxenes. Composition of pigeonites ranges from $En_{52}Fs_{45}Wo_3$ to $En_{28}Fs_{67}Wo_5$ in average, although the variation of the Wo contents of pigeonites (Wo_{2-7}) is large (Fig. 2a). Compositions of high-Ca pyroxenes occurring as discrete grains and lamellae range from $En_{37-39}Fs_{20}Wo_{41-43}$ to $En_{24}Fs_{34}Wo_{42}$, although their Wo contents (Wo_{37-43}) also vary (Fig. 2a). The Wo contents of primary high-Ca pyroxenes in a ferroan Pig-eucritic clast is about 35–36 mole % (Fig. 2a). Al_2O_3 and Cr_2O_3 of host pigeonites in Pig-eucritic clasts are lower than those in other lithic clasts (Fig. 3). Plagioclases in Pig-eucritic clasts are $An_{95}Ab_5$ to $An_{86}Ab_{14}$, and orthoclase contents are less than 0.5 mole %. The anorthite contents of plagioclases are relatively constant (Fig. 6); their chemical trend is shown by the arrow A in Fig. 6. Chromites in Pig-eucritic clasts range from $Chr_{72}Sp_{17}Us_{11}$ to $Chr_{45.5}Sp_8Us_{46.5}$, nearly the same as those in IPig-eucritic clasts (Fig. 4). They form a compositional trend from TiO_2-poor to TiO_2-rich together with chromites in Hyp-eucritic and IPig-eucritic clasts as shown in Fig. 4 by dotted arrow. Fe-metal in a magnesian Pig-eucritic clast is rich in Ni and Co whereas that in a ferroan Pig-eucritic clast is poor in Ni and Co (Fig. 5a). Troilites in Pig-eucritic clasts are very rare and there is a rough tendency for troilite/Fe-metal volume ratios to decrease from diogenitic clasts to Pig-eucritic clasts. Ilmenites are commonly observed in Pig-eucritic clasts whereas they are nearly absent in diogenitic, Hyp-eucritic and coarse-grained IPig-eucritic clasts.

Fa-Hd-Trid-Pl clasts include fayalitic olivine and tridymite instead of ferrous low-Ca pyroxenes. Composition of fayalitic olivine is $Fo_{10-14}Fa_{86-90}$ (Fig. 2a), and are the most ferroan among all known howardites and eucrites (DELANEY *et al.*, 1980; FUHRMAN and PAPIKE, 1981). Hedenbergitic pyroxenes are $En_{16-19}Fs_{40-43}Wo_{41}$. As they are free of any exsolution lamella or bleb, their composition may be primary. Plagioclases are $An_{78-85}Ab_{15-21}$, and the orthoclase contents are high (0.5–1.0 mole %). They seem to form a trend together with plagioclases in Pig-eucritic clasts as shown in Fig. 6 by the arrow A. Ilmenites are a main oxide mineral in Fa-Hd-Trid-Pl clasts, and are nearly pure ilmenite $FeTiO_3$ although they include small amounts of MgO and MnO. Chromite occurs as thin film included in a large chromite grain, and may not be a primary phase. Composition of the chromite deviates from the trend of primary chromites in eucritic clasts and is rich in Cr_2O_3 and poor in TiO_2 (Fig. 4). Whitlockite and troilite occur sometimes although Fe-metal is seldom observed. The Fa-Hd-Trid-Pl clasts show igneous texture, and are considered to be products of latest-stage differentiates of HED magmas.

Magnesian Ol-Px-Pl clasts are rare in Y-7308. As they are not so coarse-grained as diogenitic, Hyp-eucritic and coarse-grained IPig-eucritic clasts, they are probably not cumulate nor residual rocks. Rather, they may be solidified products of magnesian magmas or aggregates of microphenocrysts including trapped liquid which crystallized as plagioclase or pyroxene. Olivines are $Fo_{65-73}Fa_{27-35}$ (Fig. 2b) and almost homogeneous in a clast, but olivines in a clast show slight MgO-FeO zonation. Orthopyroxenes are $En_{66-72}Fs_{26-31}Wo_{2-3}$, and show the same range as orthopyroxenes in diogenitic and Hyp-eucritic clasts. High-Ca pyroxenes are similar in composition to those in diogenitic and Hyp-eucritic clasts although they are slightly more magnesian in magnesian Ol-Px-Pl clasts (Fig. 2b). Plagioclases are $An_{86-94}Ab_{6-13}$ and the orthoclase contents are less than 0.7 mole %. Chromite in a magnesian Ol-Px-Pl clast is $Chr_{63}Sp_{25.5}Us_{11.5}$, and deviates in composition from the trend of chromites in eucritic clasts (Fig. 4). Fe-metals are rich in Ni (1.8–4.3 wt%) and an Fe-metal with 4.3 wt% Ni includes a small taenite grain with 55.5 wt% Ni. The Co contents of Fe-metals are

0.36 to 0.46 wt%, higher than those in eucritic clasts and lower than those in diogenitic clasts (Fig. 5a).

A magnesian Ol-Px clast, the unmelted part of clast No. 7, might have been originally a coarse-grained rock consisting mainly of orthopyroxene and olivine, and it could be a fragment of cumulate or residual rocks formed in the interior of HPB. Compositions of olivine and orthopyroxene in the clast are $Fo_{72}Fa_{28}$ and $En_{74}Fs_{25}Wo_1$, respectively. The Wo contents of the orthopyroxene is lower than those in diogenitic clasts (Fig. 2b).

7.2. *Hypocrystalline to holohyalline materials*

The CaO and Al_2O_3 contents of glassy spherules and fragments are plotted on a line connecting average diogenites and average noncumulate eucrite compositions (Fig. 7b), whereas their MgO contents deviate slightly from the connecting line (Fig. 7a). This suggests that the original materials of glassy spherules and fragments were breccias

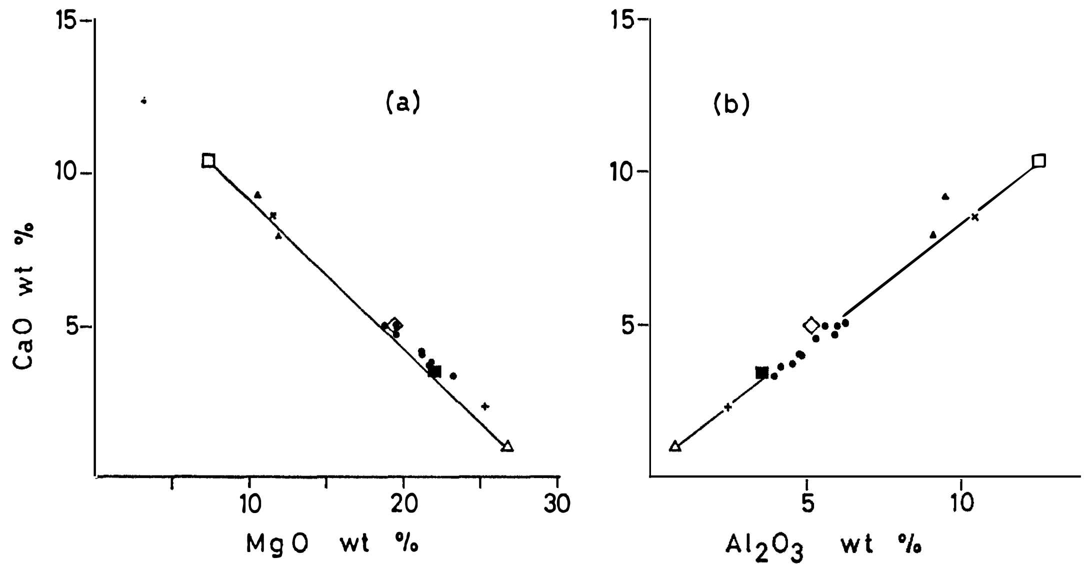

Fig. 7. CaO contents plotted against MgO contents (a) and Al_2O_3 contents (b), for glassy spherules and fragments (●), black glassy fragment No. 7′ (▲), bulk vitrophyric clast No. 13 (◇), bulk Pig-eucritic clast No. 1 (×), bulk chondrule-like material No. 71 (+), bulk Y-7308 (■, YAGI et al., 1978), average noncumulate eucrites (□, DODD, 1981), and average diogenites (△, DODD, 1981).

or regoliths including magnesian olivines in addition to eucritic and diogenitic components (Fig. 8). Glassy spherules and fragments except No. 7′ glass show relatively uniform compositions in spite of their small sizes. They are similar to the whole rock composition of Y-7308, but tend to deplete slightly in diogenitic and magnesian olivine components (Figs. 7 and 8). This tendency is also recognized for other howardites (NOONAN, 1974), and suggests that most glassy spherules and fragments represent not only the bulk compositions of breccias or regoliths but also the compositions of mixtures of matrix materials and fine-grained mineral fragments, which could easily melt by shocks (NOONAN, 1974).

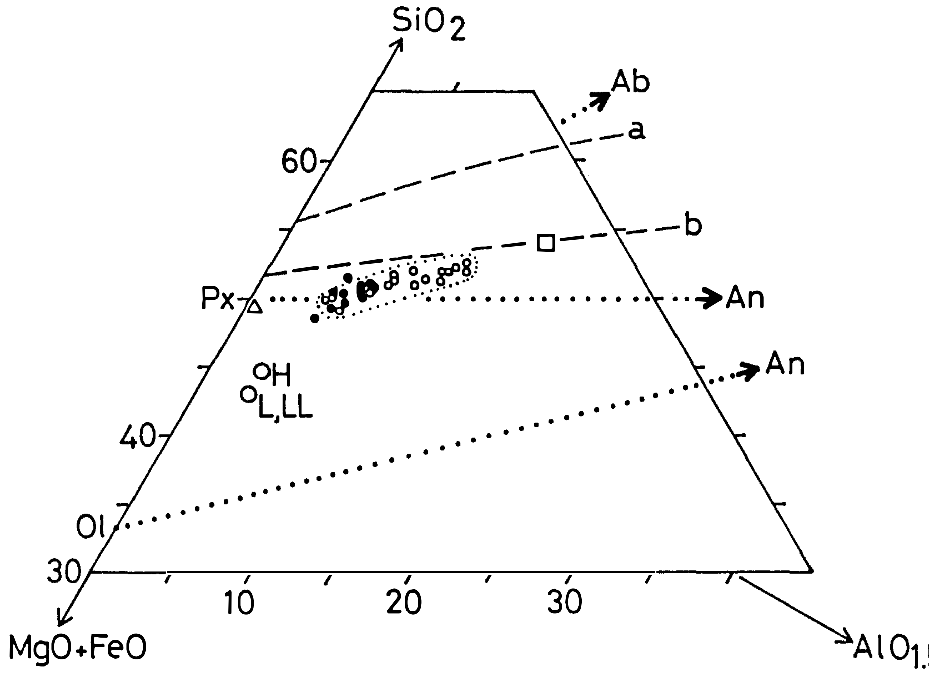

Fig. 8. *SiO_2-($MgO+FeO$)-$AlO_{1.5}$ plot (in mole ratio) of howardites (○, MASON et al., 1979, polymict breccias), glassy spherules and fragments (●) in Y-7308, average noncumulate eucrites and diogenites (□ and △, respectively, DODD, 1981), and average H and L(LL) chondrites (○, MASON, 1962). Ab, An, Px and Ol are albite, anorthite, low-Ca pyroxene and olivine, respectively. Dashed lines a and b are liquidus field boundaries of forsterite-anorthite-silica system between silica-mineral and pyroxene liquidus fields and between pyroxene and olivine liquidus fields, respectively (ANDERSEN, 1915).*

Vitrophyric clasts are compositionally similar to the glassy spherules and fragments (Fig. 7). Therefore, the original melts of the vitrophyric clasts were probably formed by shocks from materials similar to those for the glassy spherules and fragments. The difference in texture and crystallinity between them might have been explained as follows: The glassy spherules and fragments may be formed from melt droplets splashed from shocked breccias or regoliths and impact-melt lakes, which were produced from the breccias and/or regoliths similar to Y-7308 in chemical compositions. The melts in shock-melt lakes tended to cool more slowly than the splashed melt droplets, and therefore crystallized pyroxene laths or quenched crystals. After consolidation of the shock-melt lakes as vitrophyric rocks, their fragmentation resulted in the vitrophyric clasts in Y-7308. Compositions of pyroxene laths and groundmass glasses in vitrophyric clasts are plotted in Fig. 9, together with the bulk composition of clast No. 13. The bulk composition represents the composition of original melts from which pyroxene laths crystallized, and the residual melts quenched as the groundmass glasses. The Al_2O_3 and Cr_2O_3 contents of pyroxenes in vitrophyric clasts show remarkable zonation from magnesian core to ferroan rim, and form a compositional range different from those in holocrystalline lithic clasts (Fig. 3).

Chondrule-like materials showing porphyritic textures have bulk compositions similar to pyroxene-olivine porphyritic chondrules in unequilibrated chondrites (IKEDA,

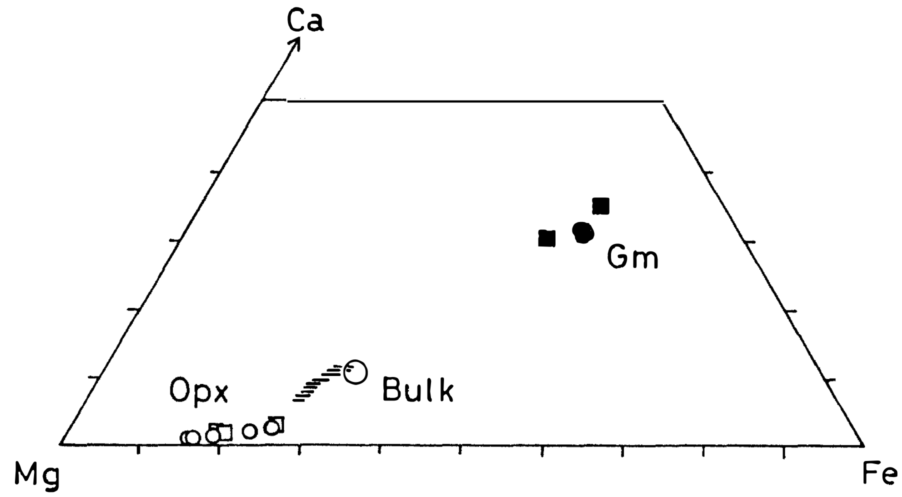

Fig. 9. Compositions (in atomic ratio) of orthopyroxenes (Opx), groundmass glasses (Gm) in two vitrophyric clasts (circles: clast No. 13, squares: clast No. 28), and bulk clast No. 13 (Bulk). Shaded area is the compositional range of glassy spherules and fragments.

1983). On the other hand, as shown in Fig. 7, the composition is plotted on the line extending from the region of glassy spherules and fragments towards the composition of the olivine- and low-Ca pyroxene-rich components. In addition, the Al_2O_3 and Cr_2O_3 contents of low-Ca pyroxenes in chondrule-like materials are plotted in the same range as those in vitrophyric clasts (Fig. 3). Therefore, there are two possibilities for the origin of chondrule-like materials: (a) Derivation from chondritic materials by their disaggregation; and (b) they crystallized in shock-melt lakes whose compositions are rich in magnesian olivine and low-Ca pyroxene components, and subsequent fragmentation and rounding resulted in chondrule-like materials.

7.3. Mineral fragments

Orthopyroxene fragments ranging from $En_{82}Fs_{17}Wo_1$ to $En_{72}Fs_{25-26}Wo_{2-3}$ are large crystals free of any exsolution lamella of high-Ca pyroxene and are primary orthopyroxenes. The ferroan part of the compositional range coincides with that of magnesian diogenitic clasts and was derived probably by complete disaggregation from the diogenitic clasts. However, large magnesian orthopyroxene fragments do not correspond to any lithic clasts, and may have been derived from magnesian orthopyroxenites not observed in Y-7308. Orthopyroxene fragments of $En_{64-69}Fs_{28-33}Wo_{2-3}$ sometimes include blebs or lamellae of high-Ca pyroxenes and were probably derived from ferroan diogenitic, Hyp-eucritic or fine-grained IPig-eucritic clasts. Orthopyroxene fragments of $En_{56-61}Fs_{36-42}Wo_{2-3}$ include exsolution lamellae of high-Ca pyroxenes and may have been derived from IPig-eucritic clasts. Pigeonite and high-Ca pyroxene fragments are not much abundant and coincide compositionally with those in magnesian Pig-eucritic clasts.

Small olivine fragments ranging from Fo_{77} to Fo_{70} may have been derived by complete disaggregation or fragmentation from fine- or coarse-grained olivine-bearing rocks such as dunitic rocks, olivine-bearing diogenites (for example, ALHA-77256, TAKEDA, 1979), magnesian Ol-Px-(Pl) clasts, or chondrule-like materials. Large olivine fragments ranging from Fo_{88} to Fo_{71} do not correspond to any lithic clasts, and may have been derived from coarse-grained rocks such as dunitic or olivine-bearing orthopyroxenites not observed in Y-7308.

Chromite fragments show nearly the same compositional range as those in diogenitic clasts (Fig. 4). They were probably derived mainly from these clasts. Compositional ranges of Fe-metal fragments are nearly the same as those in lithic clasts, indicating that they were probably derived mainly from those lithic clasts.

8. Summary

Diogenitic clasts in Y-7308 compositionally cover all known diogenities, and may have been formed as cumulates in magma reservoirs. Hyp-eucritic and coarse-grained IPig-eucritic clasts conform to a single compositional trend, and may have been also cumulates in the same reservoirs. Fine-grained IPig-eucritic clasts may represent magnesian magmas that were rich in alkalis. The Pig-eucritic clasts represent ferrous magmas depleted in alkalis and the Fa-Hd-Trid-Pl clasts are the latest-stage products of fractional crystallization of the Na-poor ferrous magmas.

Vitrophyric clasts and glassy spherules and fragments were formed as shock-melts produced from breccias and/or regoliths similar in composition to the whole rock of Y-7308. Chondrule-like materials could be derived from chondritic materials or from shock-melts of olivine- and low-Ca pyroxene-rich materials.

Most mineral fragments of pyroxene, plagioclase, chromite and Fe-metal were probably derived from holocrystalline lithic clasts and hypocrystalline to holohyaline materials by complete disaggregation. However, large magnesian olivine and orthopyroxene fragments may need other source materials. Possible candidates are dunites and/or orthopyroxenites which may be situated in the deep interior of HPB.

Acknowledgments

We thank the National Institute of Polar Research for providing us with the meteorite samples, and Prof. M. KUBOTA for permitting us to use an EPMA.

References

ANDERSEN, O. (1915): The system anorthite-forsterite-silica. Am. J. Sci., **39**, 407–454.

BENCE, A. E. and ALBEE, A. L. (1968): Empirical correction factors for the electron microanalysis of silicates and oxides. J. Geol., **76**, 383–403.

DELANEY, J. S., NEHRU, C. E. and PRINZ, M. (1980): Olivine clasts from mesosiderites and howardites; Clues to the nature of achondritic parent bodies. Proc. Lunar Planet. Sci. Conf., 11th, 1073–1087.

DODD, R. T. (1981): Meteorites; A Petrologic-Chemical Synthesis. Cambridge, Cambridge Univ. Press, 368 p.

DUKE, M. B. and SILVER L. T. (1967): Petrology of eucrites, howardites and mesosiderites. Geochim. Cosmochim. Acta, **31**, 1637–1665.

FUHRMAN, M. and PAPIKE, J. J. (1981): Howardites and polymict eucrites; Regolith samples from the eucrite parent body. Petrology of Bholgati, Bununu, Kapoeta, and ALHA76005. Proc. Lunar Planet. Sci. Conf., 12B, 1257–1279.

IKEDA, Y. (1980): Petrology of Allan Hills-764 chondrite (LL3). Mem. Natl Inst. Polar Res., Spec. Issue, **17**, 50–82.

IKEDA, Y. (1983): Major element chemical compositions and chemical types of chondrules in unequilibrated E, O, and C chondrites from Antarctica. Mem. Natl Inst. Polar Res., Spec. Issue, **30**, 122–145.

MASON, B. (1962): Meteorites. New York, J. Wiley, 274 p.

MASON, B., JAROSEWICH, E. and NELEN, J. A. (1979): The pyroxene-plagioclase achondrites. Smithson. Contrib. Earth Sci., **22**, 27–45.

NAKAMURA, Y. and KUSHIRO, I. (1970): Compositional relations of coexisting orthopyroxene, pigeonite, and augite in a tholeiitic andesite from Hakone Volcano. Contrib. Mineral. Petrol., **26**, 265–275.

NEHRU, C. E., DELANEY, J. S., PRINZ, M., WEISBERG, M. and TAKEDA, H. (1983): Yamato-7308, an important howardite. Lunar and Planetary Science XIV. Houston, Lunar Planet. Inst., 550–551.

NOONAN, A. F. (1974): Glass particles and shock features in the Bununu howardite. Meteoritics, **9**, 233–242.

STEELE, I. M. and SMITH, J. V. (1976): Mineralogy of the Ibitira eucrite and comparison with other eucrites and lunar samples. Earth Planet. Sci. Lett., **33**, 67–78.

TAKEDA, H. (1979): A layered-crust model of a howardite parent body. Icarus, **40**, 455–470.

YAGI, K., LOVERING, J. F., SHIMA, M. and OKADA, A. (1978): Mineralogical and petrographical studies of the Yamato meteorites, Yamato-7301(j), -7305(k), -7308(l), and -7303(m) from Antarctica. Mem. Natl Inst. Polar Res., Spec. Issue, **8**, 121–141.

(Received June 18, 1984; Revised manuscript received October 20, 1984)

Appendix

Table A-1. Chemical compositions of minerals in diogenitic clasts. Px, CaPx, Mask and Chr are low-Ca pyroxene, high-Ca pyroxene, maskelynite and chromite, respectively.

	No.2 clast				No.9		No.26	No.4	
	Px	CaPx	Mask	Chr	Px	Chr	Px	Px	Chr
Na_2O	0.04	0.09	0.46	0.03	0.02	0.01	0.02	0.02	0.00
MgO	23.79	15.42	0.01	2.87	24.83	3.45	27.52	27.28	3.58
Al_2O_3	0.75	0.67	34.42	14.87	0.64	9.17	0.67	0.55	8.80
SiO_2	52.57	53.83	43.03	0.07	53.50	0.11	54.28	54.93	0.23
K_2O	0.00	0.01	0.03	0.00	0.00	0.02	0.00	0.00	0.00
CaO	1.21	21.27	18.82	0.00	1.18	0.00	0.79	0.76	0.00
TiO_2	-	0.00	-	1.24	-	0.68	-	0.15	0.35
Cr_2O_3	0.51	0.26	0.07	50.85	0.40	58.90	0.47	0.38	57.12
MnO	0.75	-	0.02	0.60	0.73	0.64	0.57	0.60	0.67
FeO	20.33	8.31	0.44	31.14	19.22	28.06	15.63	15.82	27.69
Total	99.95	99.87	97.30	101.68	100.53	101.04	99.95	100.49	98.44

Table A-2. Chemical compositions of minerals in Hyp-eucritic clasts. Pl is plagioclase and the other abbreviations are the same as those in Table A-1.

	No.6 clast					No.31			No.24	
	Px	Px	CaPx	Pl	Chr	Px	CaPx	Mask	Px	Mask
Na_2O	0.00	0.00	0.08	0.63	0.00	0.00	0.08	0.46	0.03	0.42
MgO	23.59	23.61	15.21	0.01	1.96	23.61	15.03	0.00	23.23	0.01
Al_2O_3	0.62	0.57	0.94	34.86	7.87	0.72	0.81	35.41	0.79	34.63
SiO_2	53.86	52.86	52.01	44.50	0.02	53.61	54.75	44.31	53.28	43.23
K_2O	-	0.00	-	0.01	0.00	0.00	0.00	0.02	-	0.00
CaO	1.05	1.14	21.57	19.17	0.02	1.26	21.89	19.49	1.18	19.23
TiO_2	0.33	-	0.48	0.12	3.78	-	0.00	-	0.16	-
Cr_2O_3	0.42	0.24	0.42	0.02	50.90	0.35	0.30	0.06	0.18	0.00
MnO	0.73	0.73	0.32	0.00	0.76	0.69	-	0.04	0.85	0.08
FeO	20.62	20.40	8.06	0.28	33.37	19.83	7.85	0.10	20.13	0.27
Total	101.22	99.56	99.09	99.59	98.68	100.08	100.71	99.90	99.83	97.87

Table A-3. Chemical compositions of minerals in IPig-eucritic clasts. Clasts Nos. 3 and 54 are coarse-grained type and the others are fine-grained type.

	No.3 clast					No.12					No.54	
	Px	Px	CaPx	Mask	Chr	Px	Px	CaPx	Pl	Chr	Px	CaPx
Na_2O	0.03	0.00	0.10	1.03	0.00	0.01	0.02	0.13	1.07	0.00	0.01	0.11
MgO	16.16	15.89	12.21	0.01	0.70	19.43	19.07	13.58	0.00	1.52	20.80	14.38
Al_2O_3	0.43	0.36	0.75	33.98	5.23	0.36	0.45	0.90	34.06	7.37	0.49	0.74
SiO_2	50.77	50.02	50.43	45.68	0.08	52.34	50.70	51.15	44.33	0.10	52.37	51.94
K_2O	0.00	-	-	0.07	0.01	-	-	-	0.02	0.01	-	-
CaO	1.30	1.23	20.31	18.18	0.02	1.20	1.32	20.67	18.11	0.08	1.12	21.09
TiO_2	-	0.34	0.27	-	13.98	0.32	0.30	0.56	0.00	5.02	0.14	0.24
Cr_2O_3	0.19	0.11	0.24	0.00	35.65	0.46	0.14	0.20	0.00	49.13	0.39	0.54
MnO	1.03	0.98	0.49	0.01	0.70	1.01	0.78	0.58	0.00	0.75	0.85	0.46
FeO	29.90	29.52	12.85	0.13	43.40	25.79	24.99	11.58	0.27	34.72	24.10	10.40
Total	99.81	98.44	97.64	99.10	99.78	100.92	97.78	99.35	97.87	98.69	100.27	99.88

	No.54		No.40				No.301			No.304			
	Pl	Chr	Px	Px	Pl	Chr	Px	CaPx	Pl	Px	CaPx	Pl	Chr
Na_2O	0.65	0.03	0.00	0.00	1.12	0.00	0.00	0.11	1.21	0.00	0.10	1.89	0.00
MgO	0.02	2.08	19.69	19.44	0.00	1.56	19.26	13.79	0.06	19.29	13.64	0.06	1.30
Al_2O_3	34.81	8.99	0.47	0.50	34.22	7.08	0.57	1.28	33.91	0.52	1.13	33.17	9.07
SiO_2	45.36	0.06	51.21	52.45	44.91	0.00	51.39	50.89	45.81	51.05	51.11	47.74	0.08
K_2O	0.02	-	0.03	0.02	0.05	0.00	-	-	-	-	-	0.12	0.02
CaO	19.05	0.00	1.20	1.34	18.42	0.24	1.61	20.52	17.99	1.83	20.42	16.85	0.03
TiO_2	0.04	3.21	0.32	0.48	-	5.26	-	-	-	-	-	0.09	3.38
Cr_2O_3	0.13	52.98	0.58	0.36	0.09	50.86	-	-	-	-	-	0.00	52.06
MnO	-	0.71	0.88	0.78	0.00	0.62	-	-	-	-	-	-	0.71
FeO	0.14	32.25	25.90	25.43	0.29	34.51	25.86	13.15	0.49	26.52	12.49	0.84	33.68
Total	100.24	100.31	100.29	100.80	99.09	100.12	98.68	99.73	99.46	99.21	98.87	100.76	100.35

	No.65					No.9'			No.68			
	Px	CaPx	Pl	Chr	SiO_2	Px	CaPx	Pl	Px	CaPx	CaPx	Pl
Na_2O	0.00	0.14	1.39	0.04	0.10	0.00	0.10	1.12	0.00	0.07	0.12	1.21
MgO	17.75	13.09	0.01	1.14	0.07	23.01	15.67	0.10	23.97	11.32	15.46	0.04
Al_2O_3	0.32	0.98	34.40	7.29	0.39	0.31	0.81	34.31	0.37	0.69	0.56	34.23
SiO_2	50.75	50.85	45.98	0.10	97.34	54.10	52.59	46.31	52.82	50.52	52.09	45.91
K_2O	-	-	0.04	-	-	-	-	-	-	-	-	0.07
CaO	1.16	20.09	17.92	0.08	0.08	1.99	20.13	18.08	1.32	19.88	21.73	18.19
TiO_2	0.37	0.58	0.02	5.53	0.09	-	-	-	0.12	0.55	0.19	0.10
Cr_2O_3	0.20	0.46	0.00	48.31	0.08	-	-	-	0.15	0.23	0.14	0.10
MnO	1.33	0.50	0.05	0.78	0.00	-	-	-	0.66	0.60	0.31	0.00
FeO	28.07	12.27	0.21	34.97	0.90	19.35	9.98	0.34	19.96	15.91	8.22	0.33
Total	100.42	98.96	100.02	98.24	99.02	98.76	99.28	100.27	99.37	99.78	98.82	100.19

Table A-4. Chemical compositions of minerals in Pig-eucritic clasts.

	No.1 clast											
	Bulk	Px-Bulk	Px	Px	CaPx	CaPx	CaPx	CaPx	Pl	Pl	Chr	Chr
Na_2O	0.35	0.03	0.02	0.02	0.13	0.14	0.09	0.13	0.94	1.05	0.02	0.00
MgO	11.44	16.99	16.77	16.73	13.06	13.24	13.10	13.15	0.00	0.02	1.22	1.03
Al_2O_3	10.54	0.36	0.32	0.26	0.92	0.98	0.75	0.83	34.50	34.19	3.82	7.75
SiO_2	48.37	51.69	52.05	51.00	51.28	51.55	51.12	50.37	44.61	45.07	0.03	0.11
K_2O	0.03	-	0.00	0.00	0.00	0.00	0.00	0.00	0.07	0.06	0.00	-
CaO	8.52	4.59	1.22	2.01	20.34	20.41	20.91	20.51	18.40	18.25	0.05	0.03
TiO_2	0.44	0.41	0.35	-	0.70	-	-	0.66	-	0.00	17.09	6.60
Cr_2O_3	0.49	0.25	0.06	0.11	0.28	0.37	0.25	0.32	0.00	0.01	31.98	46.46
MnO	-	-	0.78	0.88	0.53	0.42	0.44	0.52	0.08	0.01	0.68	0.52
FeO	19.33	26.73	29.55	28.23	12.74	12.40	12.39	12.18	0.40	0.24	45.30	37.10
Total	99.51	101.05	101.49	99.24	100.05	99.51	99.05	98.68	99.00	98.90	100.16	99.60

	No.1		
	Chr	Il	Il
Na_2O	0.00	0.02	0.00
MgO	1.22	1.52	1.40
Al_2O_3	8.17	0.14	0.16
SiO_2	0.01	0.07	0.00
K_2O	-	0.00	-
CaO	0.03	0.07	0.02
TiO_2	7.32	52.82	53.45
Cr_2O_3	43.14	0.62	0.65
MnO	0.62	0.82	0.99
FeO	38.28	44.96	44.38
Total	98.78	101.05	101.04

	No.27					No.32				No.35		
	Px	CaPx	CaPx	CaPx	Pl	Px	CaPx	Pl	Il	Px	CaPx	Chr
Na_2O	0.01	0.12	0.09	0.09	1.13	0.01	0.08	0.62	0.00	0.03	0.08	0.00
MgO	13.61	10.72	10.78	11.24	0.00	14.87	12.10	0.01	0.77	12.96	11.01	0.74
Al_2O_3	0.29	0.82	0.79	0.80	33.27	0.21	0.23	34.01	0.06	0.19	0.83	8.49
SiO_2	49.46	50.32	49.71	50.90	44.87	50.98	49.98	44.74	0.22	49.62	49.78	0.06
K_2O	0.00	0.00	0.00	-	0.07	-	-	0.03	0.01	-	-	0.00
CaO	0.97	19.58	18.56	20.04	17.88	0.77	20.12	18.71	0.07	3.16	19.75	0.09
TiO_2	0.36	0.62	0.69	0.58	-	0.05	0.37	0.00	51.26	0.27	0.64	5.25
Cr_2O_3	0.16	0.40	0.28	0.21	0.00	0.01	0.15	0.06	0.33	0.10	0.43	47.41
MnO	1.35	0.67	0.62	0.50	0.00	0.99	1.03	0.11	0.93	0.99	0.44	0.72
FeO	35.23	15.94	16.48	15.12	0.19	32.63	14.27	0.37	45.26	32.28	15.37	37.93
Total	101.45	99.21	98.01	99.48	97.42	100.51	98.33	98.68	98.91	99.60	98.33	100.69

	No.35		No.55					No.56				
	Il	Il	Px-Bulk	Px	Px	CaPx	Pl	Px	CaPx	Pl	Chr	Il
Na_2O	0.00	0.00	0.08	0.01	0.00	0.05	1.26	0.01	0.10	1.30	0.00	0.00
MgO	1.05	0.43	7.82	9.07	8.93	8.15	0.00	18.34	13.25	0.02	1.48	1.98
Al_2O_3	0.11	0.06	0.75	0.25	0.27	0.59	33.98	0.28	1.00	33.90	8.25	0.08
SiO_2	0.10	0.12	49.11	47.15	49.26	50.02	46.60	50.92	52.03	45.77	0.00	0.03
K_2O	-	0.00	-	-	-	-	0.08	-	-	0.04	0.00	0.01
CaO	0.04	0.26	15.99	1.79	2.88	19.59	17.92	1.16	20.05	18.10	0.02	0.03
TiO_2	52.31	52.70	1.08	0.38	0.32	0.42	0.06	0.18	0.85	0.00	3.96	53.42
Cr_2O_3	0.12	0.11	0.30	0.00	0.15	0.41	0.00	0.22	0.35	0.00	50.82	0.21
MnO	0.87	0.92	-	1.46	1.39	0.54	-	0.93	0.48	0.00	0.59	0.95
FeO	44.64	44.88	23.34	38.27	38.22	20.52	0.24	28.16	12.50	0.36	33.44	44.22
Total	99.24	99.98	98.48	98.39	101.41	100.29	100.14	100.20	100.62	99.50	98.56	100.92

	No.61				No.62		No.64				No.76'	
	Px	CaPx	Pl	Il	Px	CaPx	Px	CaPx	Pl	SiO_2	Px.	Px
Na_2O	0.06	0.09	1.47	0.02	0.02	0.11	0.02	0.01	1.11	0.20	0.00	0.00
MgO	11.25	9.58	0.06	0.60	12.31	10.29	12.72	10.63	0.02	0.00	11.19	11.16
Al_2O_3	0.33	0.58	33.65	0.11	0.29	0.85	0.16	0.87	33.60	0.49	0.23	0.23
SiO_2	49.82	50.31	46.79	0.11	49.10	50.35	51.39	50.02	45.67	99.24	50.20	49.61
K_2O	-	-	0.11	-	-	-	-	-	0.04	-	-	-
CaO	2.35	17.41	17.30	0.19	1.00	19.90	1.15	19.91	17.92	0.08	1.62	1.31
TiO_2	0.33	0.42	0.00	53.43	0.46	0.73	0.24	0.24	0.07	0.25	0.27	0.61
Cr_2O_3	0.17	0.26	0.04	0.12	0.03	0.30	0.07	0.18	0.02	0.00	0.00	0.00
MnO	1.01	0.63	0.02	0.91	1.27	0.55	1.16	1.30	0.00	0.00	1.25	1.11
FeO	35.17	20.89	0.59	45.64	35.56	16.70	34.62	16.35	0.08	0.03	36.07	36.41
Total	100.49	100.17	100.02	101.13	100.05	99.77	101.52	99.51	98.54	100.29	100.78	99.98

	No.76'		No.73						No.305			No.306
	CaPx	Pl	Px	Px	CaPx	CaPx	Pl	Pl	Px	Px	Pl	Px
Na_2O	0.08	1.44	0.00	0.04	0.06	0.05	1.29	1.23	0.00	0.00	0.52	0.00
MgO	9.81	0.04	12.13	12.30	10.45	10.23	0.01	0.03	11.65	12.15	0.02	12.32
Al_2O_3	0.65	33.31	0.15	0.17	0.71	0.62	34.33	34.33	0.26	0.28	34.89	0.20
SiO_2	51.66	47.52	51.12	47.98	51.02	50.58	46.53	47.21	48.74	49.28	43.76	48.73
K_2O	-	0.10	-	-	-	-	-	-	-	-	0.06	-
CaO	19.32	17.69	1.30	1.48	19.78	19.80	17.84	18.04	2.31	1.36	18.90	1.40
TiO_2	0.52	0.00	-	0.13	-	0.53	-	-	-	-	0.00	-
Cr_2O_3	0.20	0.00	-	0.10	-	0.14	-	-	-	-	0.00	-
MnO	0.58	0.06	-	1.04	-	0.46	-	-	-	-	-	-
FeO	17.90	0.43	35.00	35.22	17.25	17.12	0.23	0.49	35.91	37.11	1.10	34.36
Total	100.70	100.58	99.70	98.47	99.26	99.54	100.25	101.34	98.86	100.17	99.24	97.02

	No.306		No.307		
	CaPx	Pl	Px	CaPx	Pl
Na_2O	0.11	1.24	0.00	0.08	0.95
MgO	10.11	0.03	17.22	13.41	0.08
Al_2O_3	1.25	34.17	0.36	0.85	34.62
SiO_2	50.51	46.22	50.47	50.90	45.42
K_2O	-	-	-	-	-
CaO	19.62	18.17	1.47	20.07	18.94
TiO_2	-	-	-	-	-
Cr_2O_3	-	-	-	-	-
MnO	-	-	-	-	-
FeO	16.97	0.58	28.33	12.25	0.63
Total	98.57	100.42	97.85	97.56	100.64

Table A-5. Chemical compositions of minerals in Fa-Hd-Trid-Pl clasts.

	No.46 clast										No.60		No.60	
	Ol	Ol	CaPx	CaPx	Pl	Pl	Chr	Il	SiO_2	SiO_2	Ol	CaPx	Pl	SiO_2
Na_2O	0.02	0.03	0.10	0.10	2.24	1.60	0.00	0.01	0.13	0.14	0.00	0.12	2.30	0.09
MgO	4.13	4.29	5.19	5.16	0.00	0.00	0.09	0.20	0.00	0.00	5.38	6.08	0.03	0.02
Al_2O_3	0.02	0.00	0.75	0.83	31.44	33.29	3.64	0.12	0.52	0.64	0.03	0.74	32.55	0.53
SiO_2	31.21	29.88	48.68	49.49	49.18	46.94	0.19	0.07	98.19	99.67	30.66	48.87	48.61	97.99
K_2O	-	-	-	-	0.19	0.12	-	-	-	-	-	-	0.22	-
CaO	0.07	0.07	18.44	18.32	15.14	16.50	0.00	0.00	0.03	0.02	0.12	18.60	15.89	0.08
TiO_2	0.13	0.02	0.74	0.70	0.00	0.16	6.41	52.79	0.04	0.18	0.09	0.51	0.09	0.00
Cr_2O_3	0.11	0.05	0.36	0.30	0.00	0.11	56.93	0.07	0.06	0.09	0.05	0.36	0.00	0.05
MnO	1.78	1.80	0.77	0.79	0.01	0.02	0.57	0.99	0.07	0.05	1.70	0.98	0.00	0.00
FeO	63.33	63.12	24.74	24.76	0.22	0.52	33.50	45.42	0.06	0.07	61.52	23.33	0.63	1.11
Total	100.80	99.25	99.78	100.45	98.42	99.25	101.33	99.67	99.09	100.89	99.54	99.59	100.32	99.87

Table A-6. Chemical compositions of minerals in magnesian Ol-Px-Pl clasts (Nos. 87, 91, 509 and 526) and a magnesian Ol-Px clast (No. 7).

	No.87 clast					No.91						
	Bulk	Ol	Px	Pl	Chr	Ol	Ol	Px	Px	CaPx	CaPx	Pl
Na_2O	0.12	-	0.03	0.76	0.01	-	-	0.01	0.03	0.13	0.13	0.69
MgO	21.96	32.38	25.15	0.01	3.81	36.85	32.38	26.27	25.63	15.95	16.01	0.03
Al_2O_3	5.03	0.00	0.47	34.98	12.76	0.01	0.06	0.41	0.89	0.97	0.74	35.48
SiO_2	50.60	35.96	53.20	44.32	0.00	36.44	35.72	53.86	53.43	52.50	52.61	44.11
K_2O	0.00	-	-	0.06	-	-	-	-	-	-	-	0.05
CaO	3.17	0.00	1.36	18.76	0.00	0.03	0.05	0.89	1.57	21.47	21.94	19.11
TiO_2	0.37	-	0.18	0.00	4.51	-	-	0.05	0.12	0.21	0.34	0.00
Cr_2O_3	1.06	-	0.26	0.00	47.19	-	-	0.11	0.40	0.52	0.38	0.00
MnO	-	0.66	0.56	0.00	0.58	0.41	0.06	0.78	0.61	0.26	0.38	0.00
FeO	16.54	31.04	18.66	0.61	31.42	24.92	29.49	17.37	16.83	7.78	7.29	0.68
Total	98.85	100.05	99.88	99.50	100.26	98.66	98.29	99.75	99.52	99.79	99.82	100.15

	No.509		No.526		No.7	
	Ol	Pl	Px	CaPx	Ol	Px
Na_2O	0.01	1.54	0.00	0.02	0.01	0.00
MgO	33.95	0.01	23.62	15.08	36.49	27.51
Al_2O_3	0.03	32.93	0.65	0.92	0.00	0.59
SiO_2	37.25	46.69	54.25	53.55	37.64	55.64
K_2O	0.00	0.12	0.00	0.00	0.01	0.01
CaO	0.03	17.41	1.37	21.68	0.04	0.72
TiO_2	0.07	0.00	0.21	0.34	-	-
Cr_2O_3	0.07	0.00	0.18	0.35	0.01	0.28
MnO	0.58	-	-	-	0.63	0.58
FeO	28.70	0.50	19.11	7.79	26.34	16.07
Total	100.69	99.20	99.40	99.74	101.18	101.40

Table A-7. Chemical compositions of glassy spherules and fragments.

	No.7'		8	10	11	41		42-1	43	59	82	85	20-1
	Core	Rim				Core	Rim						
Na_2O	0.50	1.15	0.08	0.10	0.10	0.17	0.14	0.07	0.20	0.07	0.07	0.16	0.06
MgO	10.35	12.06	21.17	19.49	21.17	19.70	18.95	19.42	18.68	21.79	21.65	19.50	23.22
Al_2O_3	9.60	9.28	4.87	5.97	4.74	5.96	5.67	6.37	6.11	4.59	4.23	5.41	4.06
SiO_2	48.26	49.84	51.69	52.25	53.44	51.11	50.22	50.64	51.50	50.10	51.10	50.31	50.11
K_2O	0.07	0.22	0.00	0.09	0.00	0.03	0.00	0.00	0.02	0.00	0.14	0.24	0.00
CaO	9.23	7.96	4.02	4.63	4.03	4.87	5.08	5.07	4.94	3.75	3.62	4.53	3.32
TiO_2	-	-	-	-	-	-	-	-	0.33	0.21	0.21	0.20	-
Cr_2O_3	0.44	0.51	1.29	1.11	1.23	1.00	1.39	0.93	1.17	1.05	1.22	1.03	1.05
MnO	0.39	0.62	0.56	0.62	0.68	0.52	0.50	0.44	0.58	0.55	0.52	0.56	0.51
FeO	20.38	17.95	16.08	16.65	15.81	17.39	17.40	16.50	17.66	16.20	16.01	15.73	16.48
Total	99.24	99.59	99.76	100.92	101.21	100.74	99.35	99.39	101.20	98.32	98.78	97.68	98.81

Table A-8. Chemical compositions of minerals and groundmass glasses (Gm) in vitrophyric clasts.

	No.13 clast											
	Bulk	Px	Px	Px	Px	Px	Gm	Gm	Gm	Gm	relic Ol	relic SiO_2
Na_2O	0.10	0.01	0.02	0.03	0.02	0.00	0.27	0.29	0.25	0.22	0.00	0.19
MgO	19.42	29.62	25.83	27.49	31.38	31.31	4.69	4.66	4.86	4.78	36.17	0.02
Al_2O_3	5.27	0.78	2.01	1.60	1.15	0.45	13.02	13.00	13.04	12.40	0.10	0.62
SiO_2	50.25	54.84	53.44	53.67	54.43	55.55	45.56	47.71	46.86	45.18	37.01	97.55
K_2O	0.00	0.00	0.00	0.01	0.00	0.00	0.04	0.03	0.06	0.03	-	-
CaO	4.95	0.81	1.37	1.18	0.61	0.62	10.58	10.58	10.53	10.37	0.11	0.06
TiO_2	0.42	0.08	-	0.08	-	-	0.76	-	0.67	-	-	0.00
Cr_2O_3	1.55	1.09	1.71	1.59	1.16	0.88	0.50	0.49	0.57	0.49	-	0.00
MnO	-	0.44	0.52	0.79	0.59	0.46	0.60	0.66	0.58	0.57	0.52	0.13
FeO	18.83	12.11	15.81	14.72	10.64	10.66	21.63	21.42	21.40	21.32	25.45	0.68
Total	100.79	99.77	100.76	101.15	99.97	99.93	97.65	98.83	98.81	95.35	99.35	99.25

	No.28						No.58		No.302
	Px	Px	Px	Gm	Gm	Gm	Ol	Glass	Px
Na_2O	0.01	0.02	0.02	0.65	0.43	0.54	0.03	0.21	0.00
MgO	29.18	25.03	28.95	3.22	11.39	5.66	42.81	13.07	33.10
Al_2O_3	1.03	2.20	1.49	14.60	10.39	10.61	0.06	9.32	0.79
SiO_2	54.30	52.21	54.29	52.74	49.02	51.02	38.46	50.92	56.14
K_2O	0.01	0.00	0.01	0.09	0.02	0.05	-	0.02	-
CaO	0.82	1.64	0.80	10.42	7.00	9.99	0.19	6.87	0.53
TiO_2	0.05	0.20	0.08	0.64	0.43	0.69	0.08	0.15	-
Cr_2O_3	1.22	2.12	1.61	0.18	0.83	0.69	0.61	0.95	-
MnO	0.53	0.66	0.52	0.51	0.64	0.72	0.49	0.63	-
FeO	12.43	16.00	12.51	18.70	0.38	19.33	18.02	17.66	9.24
Total	99.57	100.10	100.27	101.74	99.53	99.31	100.76	99.79	99.79

Table A-9. Chemical compositions of minerals in chondrule-like materials.

	No.71 clast				No.67			No.81			
	Bulk	Ol	Ol	Px	Ol	Px	Px	Ol	Ol	Px	CaPx
Na_2O	0.10	-	-	0.01	-	0.00	0.00	-	-	0.02	0.09
MgO	25.20	36.39	30.20	30.66	43.95	33.21	30.46	35.02	39.74	28.23	14.08
Al_2O_3	2.55	0.07	0.06	0.18	0.06	0.15	1.34	0.03	0.05	0.57	1.16
SiO_2	50.86	37.99	36.03	56.84	40.01	56.91	56.21	37.12	36.80	54.76	51.35
K_2O	0.00	-	-	-	-	-	-	-	-	-	-
CaO	2.30	0.17	0.18	0.18	0.01	0.14	0.99	0.04	0.05	0.97	20.46
TiO_2	0.13	-	-	0.00	-	0.00	0.02	-	-	0.16	0.75
Cr_2O_3	1.36	-	-	0.47	-	0.20	0.92	-	-	0.58	0.40
MnO	-	0.46	0.74	0.40	0.43	0.39	0.57	0.64	0.65	0.50	0.57
FeO	16.86	25.58	33.76	12.45	17.11	10.11	10.79	27.73	21.39	14.73	10.70
Total	99.36	100.65	100.97	101.20	101.57	101.11	101.30	100.58	98.68	100.51	99.56

Table A-10. Chemical compositions of minerals and glasses in the shock-melt part of clast No. 7.

	Ol	Ol	Px	Px	Gm	Gm	Gm	relic Px
Na_2O	0.00	0.00	0.03	0.00	0.54	0.51	0.31	0.51
MgO	43.98	42.10	32.28	31.09	11.47	12.57	14.77	12.57
Al_2O_3	0.09	0.05	0.66	0.78	9.20	9.30	8.25	9.30
SiO_2	38.56	36.21	55.88	55.72	51.64	51.04	50.99	51.04
K_2O	0.01	0.00	0.00	0.01	0.05	0.06	0.04	0.06
CaO	0.12	0.17	0.50	0.29	7.75	7.36	6.15	7.36
TiO_2	-	-	-	0.26	-	-	-	-
Cr_2O_3	1.74	0.62	1.06	1.12	0.89	0.91	1.10	0.91
MnO	0.42	0.46	0.39	0.37	0.51	0.56	0.67	0.56
FeO	15.35	18.66	10.06	10.66	18.67	17.68	16.71	17.68
Total	100.26	98.27	100.86	100.29	100.73	99.98	98.99	99.98

Table A-11. Chemical compositions of mineral fragments. Nos. 1011 to 63 are olivine fragments, Nos. 79 to 24 are pyroxene fragments, Nos. 81e to 75′ are plagioclase fragments and Nos. 75 to 58′ are chromite fragments. Some mineral fragments include minor other minerals, which are shown together with major mineral fragments.

	No.1011	No.84	No.21'	No.47'	No.47	No.76	No.74	No.66	No.63	No.79	
	Ol	Ol	Ol	Ol	Ol	Ol	Ol	Ol	Ol	Px	Chr
Na_2O	0.02	-	0.00	0.02	0.01	0.01	0.01	0.02	0.00	0.02	0.00
MgO	47.92	35.75	38.93	37.55	45.90	38.82	37.40	37.12	38.91	23.05	2.99
Al_2O_3	0.06	0.03	0.01	0.00	0.08	0.03	0.00	0.03	0.02	0.76	9.60
SiO_2	38.89	36.48	36.22	36.99	38.72	37.29	36.72	36.84	37.11	52.90	0.00
K_2O	0.00	-	-	-	-	-	-	-	-	-	-
CaO	0.07	0.00	0.03	0.06	0.07	0.04	0.05	0.13	0.05	1.26	0.00
TiO_2	-	-	0.00	0.10	0.00	0.00	0.04	0.04	0.00	0.31	2.34
Cr_2O_3	0.48	-	0.09	0.04	0.00	0.12	0.00	0.00	0.03	0.32	55.74
MnO	0.32	0.61	0.35	0.65	0.44	0.59	0.77	0.52	0.59	0.70	0.45
FeO	11.50	27.36	23.52	23.87	13.81	23.84	24.87	26.11	23.09	20.97	30.03
Total	99.25	100.23	99.14	99.29	99.04	100.73	99.86	100.79	99.79	100.28	101.15

	No.48				No.21		No.53			No.44		No.44'	
	Px	Px	CaPx	CaPx	Px	CaPx	Px	CaPx	Pl	Px	CaPx	Px	CaPx
Na_2O	0.03	0.01	0.09	0.11	0.02	0.06	0.01	0.17	2.40	0.00	0.07	0.03	0.09
MgO	21.61	21.66	14.57	14.53	24.64	15.78	24.87	15.88	0.04	23.49	15.42	21.63	14.71
Al_2O_3	0.65	0.58	1.06	0.99	0.66	1.05	1.00	1.13	32.61	0.67	0.89	0.53	0.80
SiO_2	52.63	52.99	51.92	51.75	53.39	51.66	52.99	53.14	49.29	53.38	52.84	52.10	51.51
K_2O	-	-	-	-	-	-	-	-	0.12	-	-	-	-
CaO	1.14	1.34	21.46	21.48	1.21	21.13	1.74	20.99	15.74	1.46	21.14	1.60	20.28
TiO_2	0.47	0.38	0.49	0.49	0.04	0.12	0.13	0.30	0.00	0.08	0.18	0.17	0.29
Cr_2O_3	0.34	0.28	0.51	0.48	0.28	0.55	0.79	1.00	0.00	0.60	0.73	0.41	0.71
MnO	0.73	0.82	0.46	0.54	0.65	0.52	0.73	0.31	0.03	0.90	0.36	0.80	0.66
FeO	22.95	22.65	9.46	9.47	19.45	8.15	18.13	7.95	0.57	19.90	8.73	22.27	10.21
Total	100.55	100.71	100.01	99.84	100.35	99.02	100.39	100.86	100.80	100.47	100.35	99.54	99.26

	No.45				No.43'		No.49		No.50		No.93
	Px	CaPx	Pl	Chr	Px	CaPx	Px	CaPx	Px	CaPx	Px
Na_2O	0.05	0.10	0.57	0.00	0.00	0.08	0.01	0.15	0.00	0.08	0.03
MgO	20.07	14.01	0.00	1.46	19.91	13.92	24.40	16.15	23.23	15.09	24.42
Al_2O_3	0.47	0.63	35.35	9.07	0.62	0.87	0.54	0.91	0.60	0.94	0.58
SiO_2	52.03	52.39	43.57	0.06	51.89	51.51	53.87	51.89	53.32	52.14	53.41
K_2O	-	-	0.05	-	-	-	-	-	-	-	-
CaO	1.25	21.04	19.04	0.00	1.68	20.99	1.33	20.64	1.31	21.41	1.01
TiO_2	0.17	0.25	0.09	2.79	0.20	0.58	0.22	0.36	0.51	0.17	0.19
Cr_2O_3	0.37	0.75	0.00	52.12	0.45	0.56	0.35	0.67	0.55	0.63	0.24
MnO	0.91	0.59	0.05	0.74	0.83	0.37	0.58	0.41	0.86	0.33	0.66
FeO	24.73	10.50	0.29	32.49	24.01	10.38	18.82	9.14	20.84	8.56	19.15
Total	100.06	100.27	99.01	98.72	99.59	99.27	100.12	100.33	100.87	99.35	99.67

	No.92		No.98		No.90		No.81'	No.83'	No.83''	No.18	No.23
	Px	Ol	Px	CaPx	Px	Ol	Px	Px	CaPx	Px	Px
Na_2O	0.02	0.00	0.03	0.12	0.02	0.00	0.02	0.02	0.13	0.01	0.02
MgO	27.57	36.95	24.11	15.47	30.35	42.95	28.96	27.39	10.69	28.17	27.54
Al_2O_3	0.56	0.02	0.73	0.83	0.62	0.04	0.72	0.63	0.88	0.48	0.79
SiO_2	53.44	36.82	53.11	52.69	55.34	38.09	53.53	54.40	51.20	54.58	54.37
K_2O	-	-	-	-	-	-	0.00	-	-	0.00	0.00
CaO	1.10	0.06	1.46	22.24	0.63	0.10	0.87	1.18	19.78	1.34	1.16
TiO_2	0.08	-	0.04	0.20	0.04	-	-	0.00	0.62	-	-
Cr_2O_3	0.40	-	0.41	0.35	1.10	-	0.33	0.38	0.36	0.36	0.71
MnO	0.58	0.58	0.77	0.37	0.43	0.47	0.50	0.53	0.59	0.50	0.44
FeO	15.62	24.12	18.36	7.73	11.51	16.32	14.26	15.51	15.02	14.75	14.93
Total	99.35	98.55	99.02	100.01	100.04	97.96	99.18	100.05	99.26	100.68	99.95

	No.23c	No.23d	No.23e	No.23f	No.5a	No.5d	No.8'	No.24b	No.11a	No.11b	No.11c	No.36b	No.3x
	Px	Px	Px	Px	Px	Px	Px	Px	Px	Px	Px	Px	Px
Na_2O	0.02	0.02	0.00	0.02	0.02	0.00	0.04	0.03	0.00	0.00	0.00	0.05	0.06
MgO	26.91	26.48	23.99	23.19	27.42	17.05	27.84	23.31	20.11	26.05	21.61	26.40	30.29
Al_2O_3	0.77	0.50	1.08	0.86	0.85	0.41	0.94	0.66	0.45	0.90	0.77	0.94	1.13
SiO_2	54.98	54.44	53.68	53.15	54.26	51.39	54.92	53.52	52.69	54.22	52.12	53.71	55.05
K_2O	0.00	0.02	0.00	0.01	0.01	0.00	0.00	0.00	0.02	0.01	0.01	-	0.00
CaO	1.28	0.90	1.91	2.05	1.07	2.43	1.40	1.50	1.46	1.54	1.25	1.63	0.97
TiO_2	-	-	-	-	-	-	-	-	-	-	-	0.03	-
Cr_2O_3	0.75	0.33	0.67	0.59	0.53	0.08	0.48	0.45	0.35	0.43	0.29	0.63	0.94
MnO	0.53	0.60	0.74	0.61	0.49	1.05	0.48	0.84	0.81	0.68	0.79	0.66	0.49
FeO	15.67	17.42	19.00	19.96	15.84	28.72	14.76	20.99	24.36	16.52	23.39	15.54	11.16
Total	100.90	100.72	101.07	100.43	100.49	101.13	100.84	101.30	100.27	100.34	100.24	99.58	100.10

	No.308	No.901	No.72		No.303		No.77b	No.24	No.81e	No.23b	No.23h	No.70	
	Px	Px	Bulk	Px	Px	Pl	CaPx	Px	Pl	Pl	Pl	Pl	SiO_2
Na_2O	0.00	0.02	0.02	0.00	0.00	0.65	0.07	0.00	1.20	1.71	0.70	0.53	0.02
MgO	19.97	31.07	17.39	17.99	20.41	0.02	11.61	27.47	0.00	0.05	0.01	0.00	0.00
Al_2O_3	0.39	0.47	0.77	0.61	0.53	35.21	0.49	0.87	33.77	32.41	35.16	34.99	0.15
SiO_2	52.60	56.05	50.52	51.24	52.88	43.71	49.71	54.37	46.20	48.06	44.99	44.25	99.17
K_2O	-	0.00	-	-	-	-	-	0.01	0.11	20.18	0.03	0.00	-
CaO	1.16	0.52	4.56	1.55	1.12	19.19	19.27	1.05	17.72	16.11	19.28	19.60	0.09
TiO_2	-	-	-	-	-	-	0.18	0.08	0.03	-	-	0.00	0.00
Cr_2O_3	-	0.27	-	-	-	-	0.01	0.59	0.01	0.02	0.00	0.00	0.00
MnO	-	0.35	-	-	-	-	0.54	0.56	0.00	0.08	0.03	-	0.00
FeO	26.11	11.48	25.99	27.78	25.81	0.70	18.12	15.06	0.64	0.45	0.09	0.17	0.19
Total	100.22	100.28	99.26	99.17	100.75	99.47	100.00	100.07	99.68	99.05	100.29	99.54	99.62

	No.75'		No.75	No.10A	No.10B	No.58'
	Pl	CaPx	Chr	Chr	Chr	Chr
Na_2O	1.15	0.09	0.02	0.00	0.00	0.01
MgO	0.02	15.55	4.99	2.83	5.07	4.24
Al_2O_3	34.34	0.80	12.08	6.49	15.65	11.37
SiO_2	46.28	54.41	0.28	0.00	0.05	0.08
K_2O	0.10	-	-	0.01	0.00	-
CaO	18.60	22.71	0.02	0.02	0.00	0.00
TiO_2	0.00	0.41	1.80	0.39	1.31	1.01
Cr_2O_3	0.00	0.20	52.85	60.82	50.88	56.15
MnO	0.07	0.57	0.63	0.68	0.46	0.53
FeO	0.25	6.65	27.65	28.76	27.29	28.06
Total	100.82	101.38	100.34	100.01	100.71	101.45

Table A-12. Chemical compositions of kamacites and a taenite in diogenitic clasts (Nos. 2 and 9), IPig-eucritic clasts (Nos. 54, 40 and 65), Pig-eucritic clasts (Nos. 27 and 56), magnesian Ol-Px-Pl clasts (Nos. 509 and 526), glassy spherule (No. 11), Olivine fragment (No. 63) and pyroxene fragments (Nos. 518, 519, 525, 14, 504, 29 and 29).

	No.2	No.9	No.54	No.40	No.65	No.27	No.56	No.509	No.509	No.526	No.11
Fe	96.6	98.5	99.7	100.0	99.3	100.0	96.5	95.3	45.0	96.3	97.3
Ni	2.5	0.46	0.04	0.0	0.18	0.00	1.7	4.5	55.5	1.8	1.9
Co	2.4	0.68	0.16	0.1	0.15	0.02	0.32	0.36	0.0	0.56	0.28
Cr	-	-	0.06	0.02	0.02	0.21	0.00	-	-	0.09	0.13
Total	101.5	99.64	99.96	100.12	99.65	100.21	98.52	100.16	100.5	98.75	99.61

	No.63	No.518	No.519	No.525	No.14	No.504	No.29	No.29
Fe	100.0	97.1	94.6	98.6	92.6	99.8	99.5	98.0
Ni	0.25	1.5	0.98	0.07	5.3	0.63	0.72	0.15
Co	0.12	0.88	2.3	1.9	1.4	0.40	0.51	0.77
Cr	0.02	0.38	0.06	0.03	0.09	0.03	-	-
TOtal	100.39	99.86	97.94	100.60	99.39	100.86	100.73	98.92

Table A-13. Chemical compositions of Fe-metal fragments. Column 20 is Fe-metal fragment (No. 506) including silicate grains.

	1	2	3	4	5	6	7	8	9	·10	11	12
Fe	100.0	98.5	92.8	98.97	96.00	99.94	99.30	95.35	95.85	99.61	97.40	99.80
Ni	0.0	0.8	6.0	0.74	2.87	0.00	0.00	3.23	1.83	0.00	1.87	0.00
Co	0.0	0.36	0.86	0.37	1.36	0.36	0.72	0.58	1.56	0.04	0.56	0.00
Cr	-	-	-	0.07	0.05	0.03	0.04	0.07	0.06	0.07	0.03	0.02
Total	100.0	99.7	99.7	100.15	100.28	100.33	100.06	99.23	99.30	99.72	99.86	99.82

	13	14	15	16	17	18	19	20
Fe	97.24	97.19	100.4	99.65	99.61	100.6	98.98	100.0
Ni	0.57	2.40	0.02	0.00	0.51	0.0	1.57	0.6
Co	1.69	0.16	0.24	0.01	0.48	0.05	0.47	0.26
Cr	0.08	0.07	0.07	0.02	0.06	0.03	0.05	-
Total	99.58	99.82	100.73	99.68	100.66	100.68	101.07	100.86

Table A-14. Chemical compositions of minerals included in Fe-metal fragment (No. 506) and troilite fragment (No. 69).

	No.506		No.69	
	Px	Qz	Px	CaPx
Na_2O	0.00	0.08	0.00	0.08
MgO	16.61	0.00	25.35	16.37
Al_2O_3	0.23	0.28	0.39	0.56
SiO_2	51.72	99.14	53.45	52.98
K_2O	0.00	0.03	-	-
CaO	1.04	0.00	1.24	22.00
TiO_2	0.81	0.17	0.04	0.00
Cr_2O_3	0.15	0.00	0.04	0.33
MnO	1.05	-	0.51	0.30
FeO	29.55	0.20	19.11	7.26
Total	100.55	99.91	100.12	99.88